OPEN ACCESS

Original research

CARD9 in neutrophils protects from colitis and controls mitochondrial metabolism and cell survival

Camille Danne ,[1,2,3] Chloé Michaudel,[1,3] Jurate Skerniskyte,[4] Julien Planchais,[1,3] Aurélie Magniez,[1,3] Allison Agus,[1,3] Marie-Laure Michel,[1,3] Bruno Lamas,[1,3] Gregory Da Costa,[1,3] Madeleine Spatz,[1,3] Cyriane Oeuvray,[2,3] Chloé Galbert,[2,3] Maxime Poirier,[1,3] Yazhou Wang,[1,3] Alexia Lapière,[1,3] Nathalie Rolhion,[2,3] Tatiana Ledent,[2] Cédric Pionneau,[5] Solenne Chardonnet,[5] Floriant Bellvert,[6] Edern Cahoreau,[6] Amandine Rocher,[6] Rafael Rose Arguello,[7] Carole Peyssonnaux,[8] Sabine Louis,[8] Mathias L Richard,[1,3] Philippe Langella,[1,3] Jamel El-Benna,[9] Benoit Marteyn,[4,10,11] Harry Sokol[1,2,3]

► Additional supplemental material is published online only. To view, please visit the journal online (http://dx.doi.org/10.1136/gutjnl-2022-326917).

For numbered affiliations see end of article.

Correspondence to
Dr Camille Danne, Université Paris-Saclay, INRAE, AgroParisTech, Micalis Institute, Jouy-en-Josas, France; camille.danne@gmail.com
Dr Harry Sokol; harry.sokol@aphp.fr

Received 8 January 2022
Accepted 4 September 2022
Published Online First 27 September 2022

Check for updates

© Author(s) (or their employer(s)) 2023. Re-use permitted under CC BY. Published by BMJ.

To cite: Danne C, Michaudel C, Skerniskyte J, *et al*. *Gut* 2023;**72**:1081–1092.

ABSTRACT

Objectives Inflammatory bowel disease (IBD) results from a combination of genetic predisposition, dysbiosis of the gut microbiota and environmental factors, leading to alterations in the gastrointestinal immune response and chronic inflammation. Caspase recruitment domain 9 (*Card9*), one of the IBD susceptibility genes, has been shown to protect against intestinal inflammation and fungal infection. However, the cell types and mechanisms involved in the CARD9 protective role against inflammation remain unknown.

Design We used dextran sulfate sodium (DSS)-induced and adoptive transfer colitis models in total and conditional CARD9 knock-out mice to uncover which cell types play a role in the CARD9 protective phenotype. The impact of *Card9* deletion on neutrophil function was assessed by an in vivo model of fungal infection and various functional assays, including endpoint dilution assay, apoptosis assay by flow cytometry, proteomics and real-time bioenergetic profile analysis (Seahorse).

Results Lymphocytes are not intrinsically involved in the CARD9 protective role against colitis. CARD9 expression in neutrophils, but not in epithelial or CD11c+cells, protects against DSS-induced colitis. In the absence of CARD9, mitochondrial dysfunction increases mitochondrial reactive oxygen species production leading to the premature death of neutrophilsthrough apoptosis, especially in oxidative environment. The decreased functional neutrophils in tissues might explain the impaired containment of fungi and increased susceptibility to intestinal inflammation.

Conclusion These results provide new insight into the role of CARD9 in neutrophil mitochondrial function and its involvement in intestinal inflammation, paving the way for new therapeutic strategies targeting neutrophils.

WHAT IS ALREADY KNOWN ON THIS TOPIC

⇒ In inflammatory bowel disease (IBD), alterations of the immune response lead to exacerbated and chronic intestinal inflammation.
⇒ Caspase recruitment domain 9 (*Card9*), one of the IBD susceptibility genes, is protective against intestinal inflammation and fungal infection; but the cell types and cellular mechanisms involved remain unknown.

WHAT THIS STUDY ADDS

⇒ Different knock-out mice showed that CARD9 expression in neutrophils, but not in lymphocytes, epithelial cells or CD11c$^+$ cells, protects against intestinal inflammation.
⇒ In the absence of CARD9, neutrophils die prematurely through apoptosis, due to a dysfunction of their mitochondria that produce excessive mitochondrial reactive oxygen species.
⇒ The survival defect of neutrophils might explain the increased susceptibility to intestinal inflammation and fungal infection in a context of *Card9* deficiency in vivo.

HOW THIS STUDY MIGHT AFFECT RESEARCH, PRACTICE OR POLICY

⇒ Understanding the role of CARD9 and neutrophils in chronic inflammation could lead to innovative therapeutic strategies targeting these key immune cells for various complex diseases.

INTRODUCTION

Inflammatory bowel disease (IBD) results from a combination of genetic predisposition, dysbiosis of the gut microbiota and environmental factors, leading to alterations in the gastrointestinal immune response and chronic inflammation.[1 2] Especially, the innate compartment of the immune system has been involved in IBD development, with a role for dendritic cells, macrophages and neutrophils.[3–6] Neutrophils, one of the most abundant and important mediators of innate immunity, are professional phagocytes that mount the acute inflammatory response and act as the first line of defence against invading pathogens.[7 8] An impaired neutrophil function may result in limited pathogen

Gut: first published as 10.1136/gutjnl-2022-326917 on 27 September 2022. Downloaded from http://gut.bmj.com/ on October 9, 2024 at Library of Vilnius University. Protected by copyright.

clearance and fuel a chronic inflammatory response with excessive lymphocyte activation. Patients with congenital disorders in neutrophil function such as chronic granulomatous disease (CGD) often develop IBD-like phenotypes.[9–12] Moreover, functional defects have been observed in neutrophils from patients with IBD, including impaired chemotaxis, migration, phagocytosis or reactive oxygen species (ROS) production.[4 5]

CARD9, one of the numerous IBD susceptibility genes, encodes an adaptor protein that integrates signals downstream of pattern recognition receptors.[13–18] Especially, CARD9 is involved in the host defence against fungi via C-type lectin sensing.[19 20] CARD9 polymorphisms in humans are associated with multiple susceptibilities including IBD,[21] whereas loss-of-function mutations are associated with invasive fungal infections caused by species such as *Candida albicans*.[21–24] CARD9 was shown to mediate its protective functions, at least in part, through the induction of adaptive Th17 cell responses.[22 23 25] *Card9*$^{-/-}$ mice are more susceptible to colitis due to impaired IL-22 production and have an increased load of gut-resident fungi.[25] Indeed, CARD9 affects the composition and function of the gut microbiota, altering the production of anti-inflammatory microbial metabolites.[26 27] However, the cell types involved in the CARD9 protective role against intestinal inflammation remain unknown.

In this work, we show that CARD9 expression in neutrophils, but not in epithelial or CD11c+cells such as dendritic cells, protects against dextran sulfate sodium (DSS)-induced colitis in mice. The absence of CARD9 impacts neutrophil capacity to contain fungal dissemination, notably by impairing neutrophil mitochondrial function and survival. Indeed, *Card9* deletion induces a basal overactivation of mitochondria, increasing the generation of mitochondrial ROS (mtROS) and leading to neutrophil apoptosis. These results provide new insight into the role of CARD9 in neutrophil mitochondrial function and its consequences in intestinal inflammation.

RESULTS

Lymphocytes have no intrinsic role in the *Card9*$^{-/-}$ susceptibility to colitis

CARD9 was previously reported to be mainly expressed in myeloid cells, especially dendritic cells, macrophages and neutrophils.[14 28] Using qRT-PCR analyses in various C57BL/6 mouse organs, we confirmed that *Card9* is mainly expressed in immune organs such as bone marrow, spleen and distal small intestine (ileum), but is low at baseline in proximal and mid small intestine, caecum, colon, stomach and liver, and not detectable in *Card9*$^{-/-}$ tissues (online supplemental figure S1A). Consistently, western-blot analysis showed the expression of CARD9 protein in bone marrow, spleen and distal small intestine of WT mice (online supplemental figure S1B). To dissect *Card9* expression at the cellular level, we sorted immune cell populations from spleen and bone marrow of WT mice. *Card9* is highly expressed in neutrophils (Ly6G$^+$CD11b$^+$ cells), macrophages (CD11b$^+$F4/80$^+$ cells), CD11c$^+$ cells, including dendritic cells, and monocytes (CD11b^{hi}F4/80$^+$ cells); but the expression is lower in innate or adaptive lymphocytes (CD3$^+$TCRγδ$^+$ lymphoid cells, CD3$^+$CD4$^+$ and CD3$^+$CD8$^+$ T cells, CD3$^-$CD19$^+$ B cells) (online supplemental figure S1C). Thus, CARD9 likely plays a major role within the myeloid immune compartment.

Previous studies from our group and others started to investigate the role of *Card9* in murine models of experimental colitis, showing that *Card9* deletion increases colitis susceptibility.[25 26 29] In order to decipher the respective roles of lymphocytes and myeloid cells in the *Card9* susceptibility to intestinal injury and inflammation, we first induced colitis with DSS in *Rag2*$^{-/-}$ and *Rag2*$^{-/-}$x*Card9*$^{-/-}$ mice that are deficient in functional T and B cells. Mice were euthanised after receiving 3% DSS in drinking water for 7 days, as the severity limit was reached for the *Rag2*$^{-/-}$x*Card9*$^{-/-}$ group. Indeed, desease severity (defined by weight loss, DAI (Disease Activity Index) score, colon length and histological score) was strongly increased in *Rag2*$^{-/-}$x*Card9*$^{-/-}$ mice compared with *Rag2*$^{-/-}$ mice (figure 1A–E). In an adoptive transfer model of colitis, in which *Rag2*$^{-/-}$ mice lacking functional lymphocytes received T cells either from WT or *Card9*$^{-/-}$ mice, no difference was observed on colitis severity (figure 1F), meaning that *Card9* expression in T cells does not impact colitis susceptibility. However, the transfer of WT T cells into *Rag2*$^{-/-}$x*Card9*$^{-/-}$ recipient mice did aggravate colitis compared with *Rag2*$^{-/-}$ simple KO recipients, with a significantly stronger weight loss (figure 1F). These results demonstrate that *Card9* mediates its protective role against colitis through the innate immunity compartment, although its role in intestinal epithelial cells cannot be ruled out.

Card9 expression in neutrophils, but not in epithelial or CD11c$^+$ cells, protects against colitis

Based on these findings, we generated conditional KO mice using the cre-lox technology, and obtained mouse strains defective for *Card9* either in epithelial cells only (Villincrex*Card9*lox line), CD11c-expressing cells only, including dendritic cells, macrophages and monocytes (CD11ccrex*Card9*lox line), or neutrophils only (Mrp8crex*Card9*lox line). To validate their phenotypes, we isolated epithelial cells from the colonic lamina propria (LP) of *Card9*^{Villincre} and *Card9*^{Villinwt} mice, or used MACS separation columns to isolate either CD11c$^+$ or Ly6G$^+$ cell fractions from spleen or bone marrow of *Card9*^{CD11cwt} and *Card9*^{CD11ccre} mice or *Card9*^{Mrp8wt} and *Card9*^{Mrp8cre} mice, respectively. We performed qRT-PCR on these cell fractions (online supplemental figure S2A), and western-blot analyses on the Ly6G$^+$ and Ly6G$^{low/-}$ fractions of *Card9*WT, *Card9*$^{-/-}$, *Card9*^{Mrp8wt} and *Card9*^{Mrp8cre} mice (online supplemental figure S2B). Results confirmed that *Card9* deletion is restricted to the expected cell types (online supplemental figure S2A,B). Purity of Ly6G$^+$CD11b$^+$ neutrophils isolated from the bone marrow of C57Bl/6 mice reached 95% by flow cytometry (online supplemental figure S2C).

We then assessed the susceptibility of these newly generated mice strains in a model of intestinal inflammation. DSS was administered for 7 days, followed by additional 5 days in which DSS was discontinued. The deletion of *Card9* in epithelial or CD11c$^+$ cells did not affect mouse susceptibility to colitis (figure 2A,B and online supplemental figure S2D). However, the deletion of *Card9* in neutrophils aggravates colitis compared with WT littermate controls, with significantly increased weight loss from day 8 (figure 2C), DAI score from day 5 (figure 2C), and histological score (figure 2E,F), as well as decreased colon length (figure 2D). Thus, the expression of *Card9* in neutrophils plays a crucial role in the protection against intestinal inflammation. The expression of myeloperoxidase (MPO), an anti-microbial enzyme abundantly expressed in neutrophils, was increased in *Card9*^{Mrp8cre} compared with *Card9*^{Mrp8wt} colon tissue at day 12, indicating a more important presence or activation of neutrophils in the absence of *Card9* (figure 2G). Similarly, the expression of the inflammatory marker lipocalin (*Lcn2*) was increased in *Card9*^{Mrp8cre} colon tissue at day 12 (figure 2H).

These results suggest that *Card9*-deficient neutrophils are efficiently recruited to the inflamed tissue but likely exhibit functional defects preventing them from adequately controlling microbial invaders and thus maintaining inflammation within the

Gut: first published as 10.1136/gutjnl-2022-326917 on 27 September 2022. Downloaded from http://gut.bmj.com/ on October 9, 2024 at Library of Vilnius University. Protected by copyright.

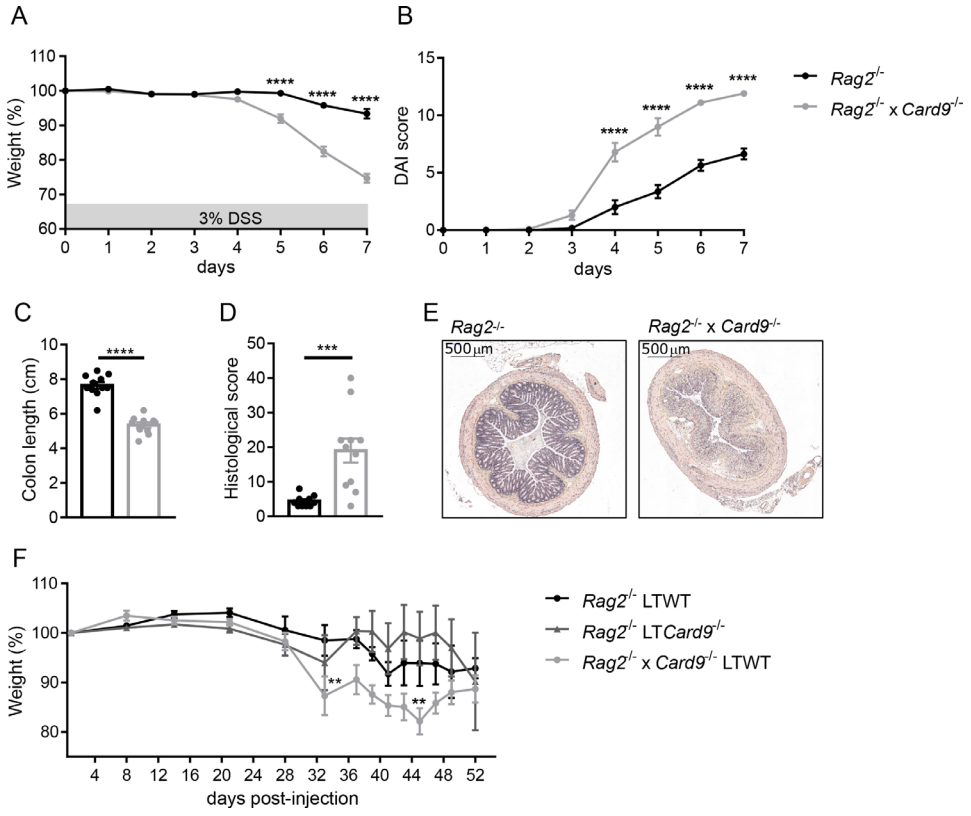

Figure 1 Lymphocytes have no intrinsic role in the *Card9*$^{-/-}$ phenotype in colitis models. (A) Weight and (B) Disease Activity Index (DAI) score of DSS-exposed *Rag2*$^{-/-}$ or *Rag2*$^{-/-}$ *x Card9*$^{-/-}$ mice. (C) Colon length and (D) histological score of colon sections at day 7. Data points represent individual mice. One representative experiment out of three. (E) Representative H&E-stained images of mid-colon cross-sections from DSS-exposed *Rag2*$^{-/-}$ (left) and *Rag2*$^{-/-}$ *x Card9*$^{-/-}$ (right) mice at day 7. Scale bars, 500 µm. (F) Weight of mice receiving naive T cells for adoptive transfer of colitis experiment. *Rag2*$^{-/-}$ received either WT or *Card9*$^{-/-}$ lymphocytes. *Rag2*$^{-/-}$ *x Card9*$^{-/-}$ mice received WT lymphocytes. Data are mean±SEM of two independent experiments. *p<0.05, **p<0.01, ***p<0.001, ****p<0.0001 as determined by two-way analysis of variance with Sidak's post-test (A, B, F) and Mann-Whitney U test (C, D). DSS, dextran sulfate sodium; LT, lymphocytes T.

intestinal mucosa. We previously showed that the gut microbiota of total *Card9*$^{-/-}$ KO lineage mice exhibit an altered production of AhR agonists compared with WT.[26] However, no difference was observed between *Card9*^{Mrp8wt} and *Card9*^{Mrp8cre} mice (online supplemental figure S2E), suggesting that this aspect of the phenotype is not intrinsically related to the role of CARD9 in neutrophils.

Card9 deletion affects the number of activated neutrophils in the inflamed colon

To investigate neutrophil function in WT mice during DSS-induced inflammation, we analysed RNA expression of the neutrophil-specific genes *Lcn2*, *Cxcr2* and *S100A8* in colon tissue at days 0, 4, 7, 9, 12 and 16 of DSS-induced colitis (figure 3A and online supplemental figure S2F). The neutrophil recruitment was maximal at day 9, corresponding to the peak of clinical inflammation, and remained high up to day 16 (figure 3A). Histological sections of the distal colon confirmed these findings (figure 3B). The fact that inflammation was higher in *Card9*^{Mrp8cre} than in *Card9*^{Mrp8wt} mice (online supplemental figure S2E), and that *Lcn2*, *Cxcr2* and *S100a8* expression at day 9 in colon tissue were similar in both genotypes (figure 3C) excludes the hypothesis of a defect of neutrophil recruitment in *Card9*^{Mrp8cre} mice. We then examined the immune cell populations recruited to the colon LP of *Card9*^{Mrp8cre} vs *Card9*^{Mrp8wt} mice at day 9 of colitis. Surprisingly, although the total number of neutrophils was similar in the two genotypes, the percentage and count of mature and activated Ly6G^{+}CD11b^{+} neutrophils was decreased in the colon LP of *Card9*^{Mrp8cre} (figure 3D,E). Moreover, the expression levels of both Ly6G and CD11b surface proteins, two major neutrophil maturation and activation markers, were significantly reduced in the overall neutrophil population, as shown by decreased MFIs (for Mean Fluorescence Intensity) (figure 3F,G). These findings suggest a structural or functional defect in neutrophils deleted for *Card9*.

Candida albicans killing capacities are impacted by *Card9* deletion in neutrophils

To investigate the defect caused by *Card9* deletion in *Card9*^{Mrp8cre} compared with *Card9*^{Mrp8wt} neutrophils, we developed several in vitro assays with Ly6G^{+} neutrophils purified from mouse bone marrow using MACS separation columns. Immunofluorescence, scanning electron microscopy (SEM) and transmission electron microscopy (TEM) analyses did not reveal noticeable structural differences between both genotypes (online supplemental figure 3). On the functional side, we tested the neutrophils ability to kill microorganisms, especially fungi, as CARD9 plays a crucial role in host defence against fungal infection in both humans and mice.[20 25] Indeed, *C. albicans* killing capacities are strongly affected by *Card9* deletion in neutrophils (figure 4). An endpoint-dilution survival assay in 96-well plates revealed that twice as many *C. albicans* cfu (colony forming unit) do survive after 24 hours co-incubation with *Card9*$^{-/-}$ or *Card9*^{Mrp8cre} neutrophils compared with Card9WT or *Card9*^{Mrp8wt}

Gut: first published as 10.1136/gutjnl-2022-326917 on 27 September 2022. Downloaded from http://gut.bmj.com/ on October 9, 2024 at Library of Vilnius University. Protected by copyright.

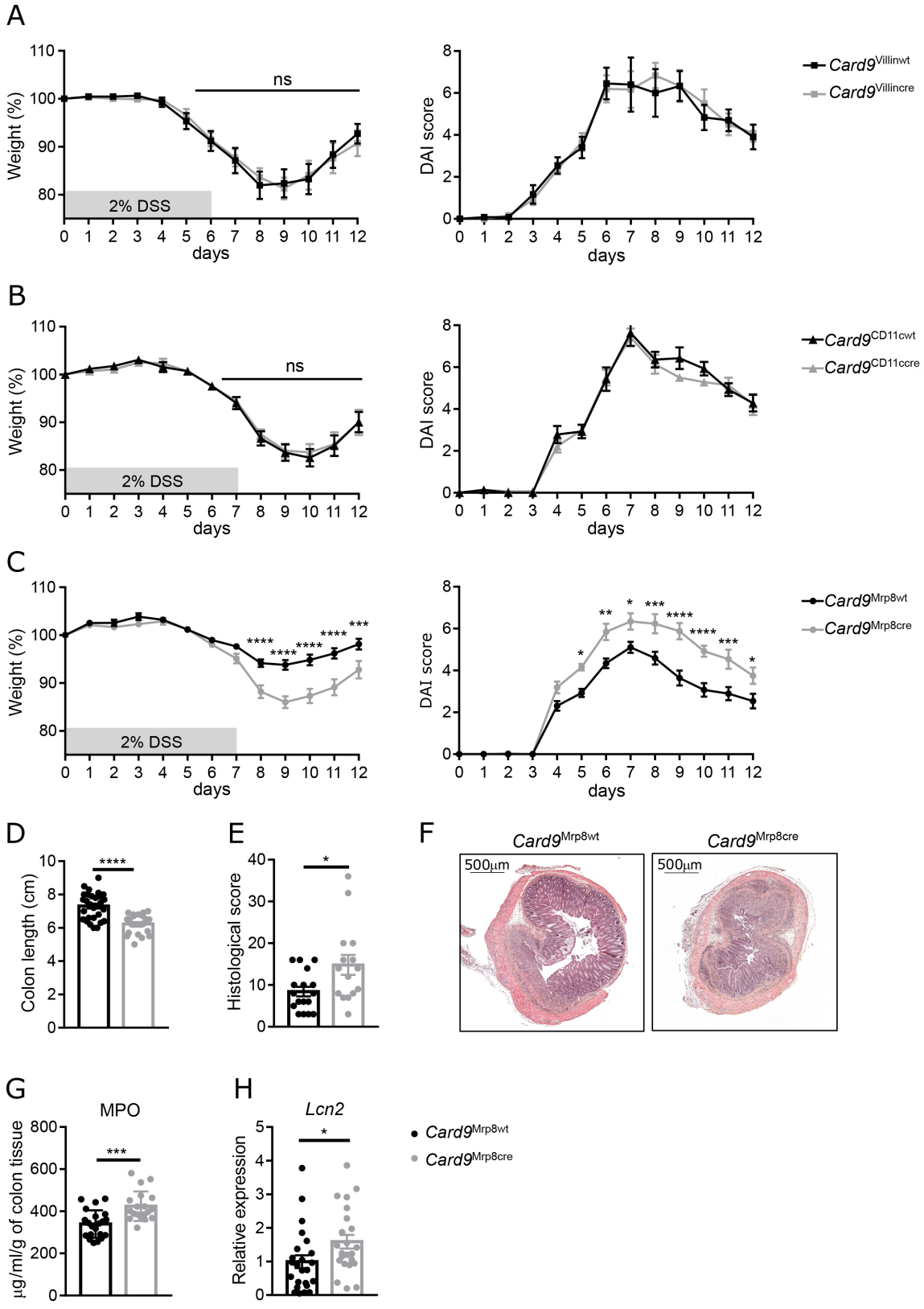

Figure 2 *Card9* expression in neutrophils, but not in epithelial or CD11c$^+$ cells, protects against colitis. (A) Weight and DAI score of DSS-exposed *Card9*^{Villinwt} or *Card9*^{Villincre} mice. (B) Weight and DAI score of DSS-exposed *Card9*^{cd11cwt} or *Card9*^{cd11ccre} mice. (C) Weight and DAI score of DSS-exposed *Card9*^{Mrp8wt} or *Card9*^{Mrp8cre} mice. (D) Colon length, (E) histological score of colon sections and (F) representative H&E-stained images of mid colon cross-sections from DSS-exposed *Card9*^{Mrp8wt} (left) and *Card9*^{Mrp8cre} (right) mice at day 12. Scale bars, 500 µm. (G) Myeloperoxidase (MPO) concentration in total colon tissue at day 12. (H) Lipocalin (*Lcn2*) expression by qRT-PCR in total colon tissue at day 12, normalised to *Gapdh*. Data points represent individual mice. Data are mean±SEM of three independent experiments. *p<0.05, **p<0.01, ***p<0.001, ****p<0.0001 as determined by two-way ANOVA with Sidak's post-test (A–C) and Mann-Whitney U test (D–H). ANOVA, analysis of variance; DAI, Disease Activity Index; DSS, dextran sulfate sodium; ns, not significant.

Gut: first published as 10.1136/gutjnl-2022-326917 on 27 September 2022. Downloaded from http://gut.bmj.com/ on October 9, 2024 at Library of Vilnius University. Protected by copyright.

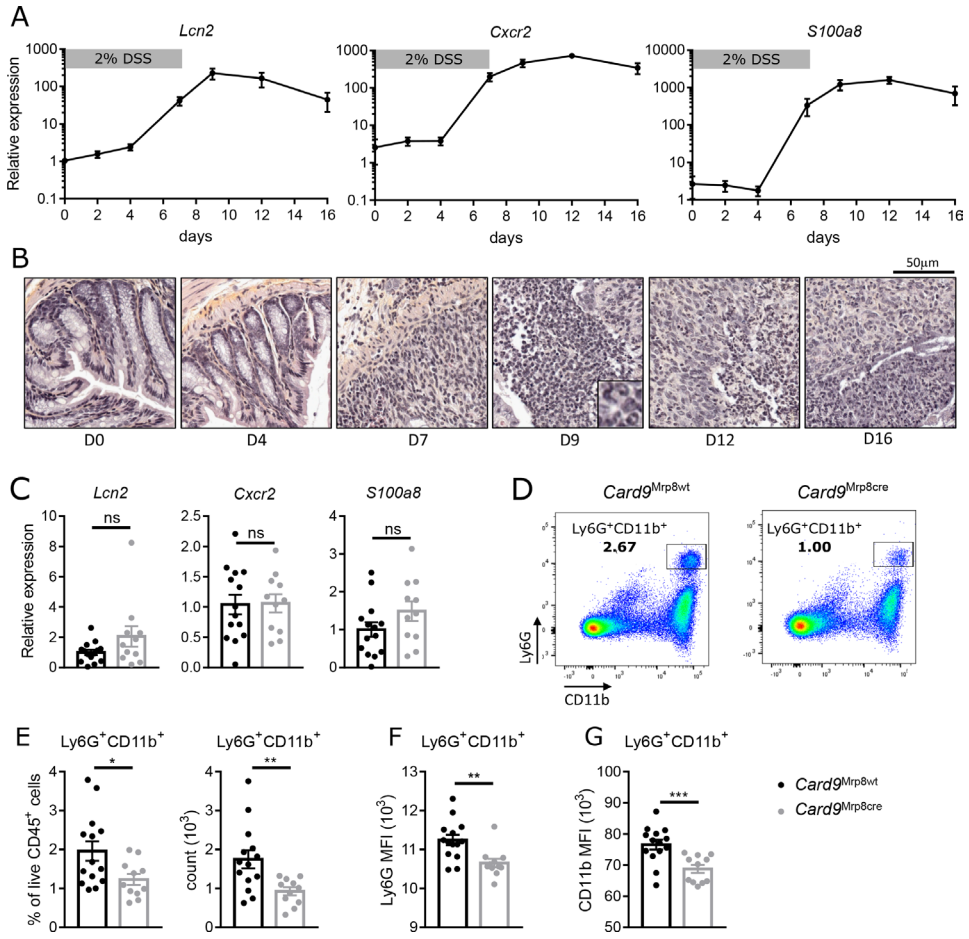

Figure 3 *Card9* deletion affects the number of mature neutrophils in the inflamed colon. (A) Relative expression of *Lcn2*, *Cxcr2* and *S1008a* in distal colon tissue of C57BL/6WT mice during a DSS colitis model relative to *Gapdh*. (B) Representative H&E-stained images of mid colon cross-sections from DSS-exposed WT mice at days 0, 4, 7, 9, 12 and 16 after DSS exposure. Scale bars, 50 µm. (C) *Lcn2*, *Cxcr2* and *S100A8* expression in total colon tissue from $Card9^{Mrp8wt}$ and $Card9^{Mrp8cre}$ mice at day 9 of DSS colitis by qRT-PCR analyses, normalised to *Gapdh*. (D) Representative flow cytometry plots of $Ly6G^+CD11b^+$ cells (neutrophils) in the colon lamina propria (LP) of DSS-exposed $Card9^{Mrp8wt}$ and $Card9^{Mrp8cre}$ mice. (E) Percentage and count of $Ly6G^+CD11b^+$ cells in the LP of DSS-exposed $Card9^{Mrp8wt}$ and $Card9^{Mrp8cre}$ mice. (F) Ly6G and (G) CD11b expression (MFI, mean fluorescence intensity) of $Ly6G^+CD11b^+$ neutrophils from $Card9^{Mrp8wt}$ and $Card9^{Mrp8cre}$ mice. Data points represent individual mice. Data are mean±SEM of two independent experiments. *p<0.05, **p<0.01, ***p<0.001 as determined by Mann-Whitney U tests. DSS, dextran sulfate sodium.

controls, respectively (figure 4A,B). A killing assay using the cfu counting method on agar plates confirmed that $Card9^{Mrp8cre}$ neutrophils have impaired abilities to kill *C. albicans* compared with $Card9^{Mrp8wt}$ (figure 4C). *Card9* deletion in neutrophils did not impact phagocytosis per se, as shown by flow cytometry experiments using fluorescein-isothiocyanate (FITC)-conjugated zymosan (from *Saccharomyces cerevisiae* cell wall), or cultures of live *C. albicans*-GFP or *E. coli*-GFP (online supplemental figure S4A,B). Moreover, we did not observe a difference in the levels of reactive oxygen species (ROS) production over time between neutrophils of the two genotypes in response to phorbol myristate acetate (PMA), a PKC-dependent neutrophil activator or zymosan, a fungal stimulus (online supplemental figure S4C,E). Even though *Card9* is involved in autophagy,[30] this cellular process did not seem to be affected by *Card9* deletion in neutrophils in vitro, as shown by the normality of p62 and LC3BII/I ratio on western-blots (online supplemental figure 4F). Similarly, in our conditions, we did not see clear differences in NETosis pattern between neutrophils deleted or not for CARD9 in response to zymosan (online supplemental figure 4H).

We, thus, followed the track of fungal killing to investigate whether the absence of *Card9* expression in neutrophils drives a general impairment of the immune system to control infection. During a DSS-induced colitis model, we detected a slight but non-significant increase in total fungi/bacteria DNA ratio at days 7 and 12 in the faeces of $Card9^{Mrp8cre}$ compared with $Card9^{Mrp8wt}$ mice (online supplemental figure S4G). These data suggest a reduced ability of $Card9^{Mrp8cre}$ mice to contain fungi expansion in the inflamed intestine. However, this effect might be difficult to point out due to the very low fungal abundance in SPF mouse microbiota. Thus, to go further and reveal a potential phenotype, we induced colitis in mice treated with a broad-spectrum antibiotic and antifongic cocktail and gavaged with *C. albicans* to expand the intestinal fungal load (figure 4D). The increased colitis severity in $Card9^{Mrp8cre}$ mice was maintained in this setting (figure 4E–G). *C. albicans* load was slightly increased (although not statistically significant) in the caecal content (figure 4H,I), colon and caecal tissues (figure 4J) of $Card9^{Mrp8cre}$ mice, and the number of cfu recovered from liver, spleen and kidney were significantly higher compared with $Card9^{Mrp8wt}$ mice (figure 4K). These results show that *Card9* expression in neutrophils is crucial to control the fungal load in the inflamed gut, the direct translocation of *C. albicans* from the gut to the liver, and to avoid its systemic dissemination.

Gut: first published as 10.1136/gutjnl-2022-326917 on 27 September 2022. Downloaded from http://gut.bmj.com/ on October 9, 2024 at Library of Vilnius University. Protected by copyright.

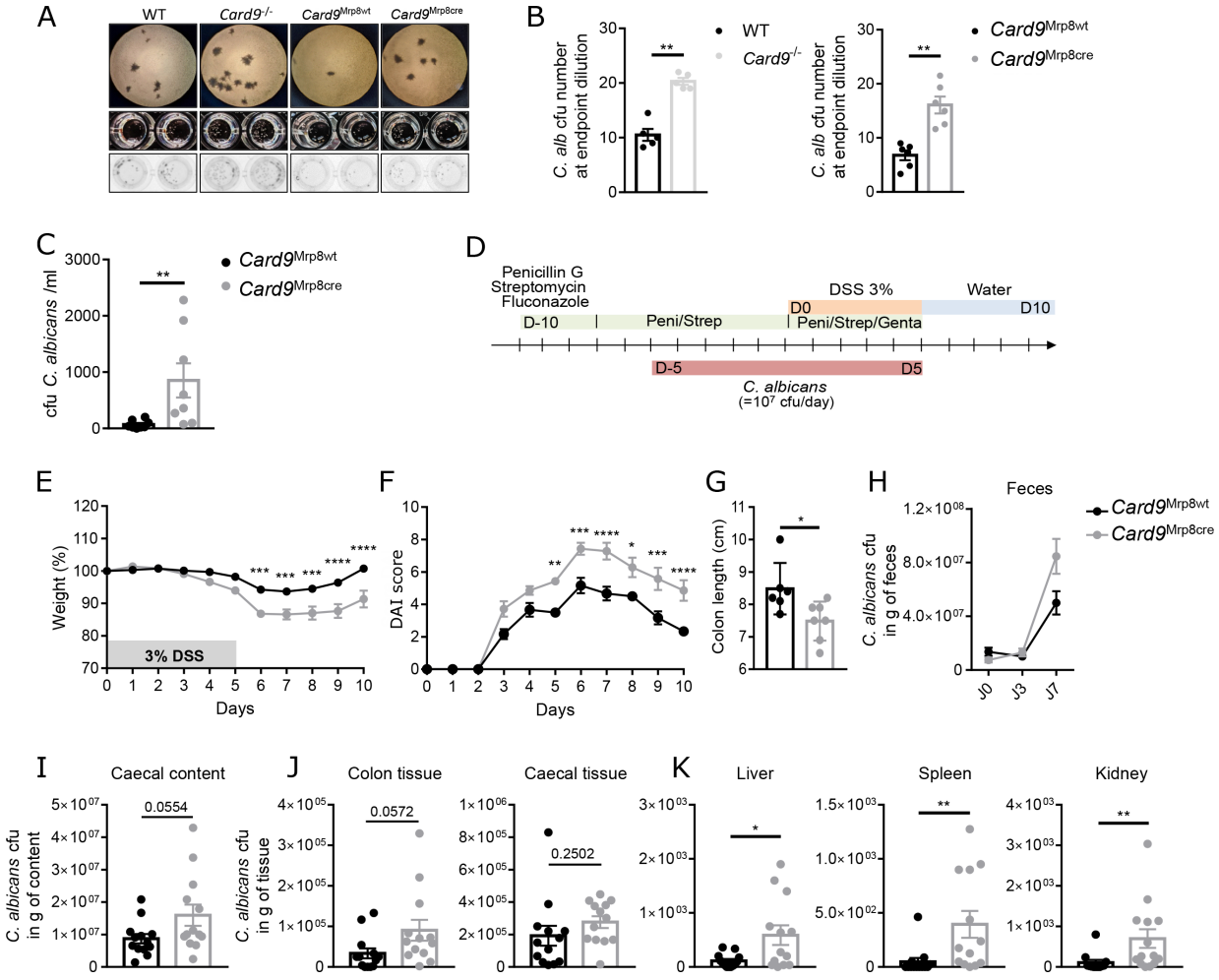

Figure 4 *Candida albicans* killing capacity is impacted by *Card9* deletion in neutrophils. (A) Representative images of *C. albicans* cfu number at the endpoint dilution after infection of *Card9*WT, *Card9*$^{-/-}$, *Card9*^{Mrp8wt} or *Card9*^{Mrp8cre} neutrophils for 24 hours, using a microscope (top) or directly showing *C. albicans* cfu in the 96-well plate, with a photography from above (middle picture) or a scan from below the plate (bottom picture). (B) *C. albicans* cfu after infection of neutrophils for 24 hours. Cfu counting was performed in 96 well plates using a microscope. Data points represent individual mice. Data are mean±SEM of three independent experiments. (C) *C. albicans* cfu number after infection of *Card9*^{Mrp8wt} or *Card9*^{Mrp8cre} neutrophils for three or 24 hours. Cfu counting was performed after plating on YEPD agar plates. Data are mean±SEM of two independent experiments. (D) Experimental design of antibiotic treatments and *C. albicans* inoculation in mice treated with 3% DSS. (E) weight, (F) DAI and (G) colon length of DSS-exposed *Card9*^{Mrp8wt} and *Card9*^{Mrp8cre} mice after colonisation with *C. albicans*. (H–K) Fungal burden in the faeces (H), caecal content (I), caecal and colon tissue (J) and liver, spleen and kidney (K) of DSS-exposed *Card9*^{Mrp8wt} and *Card9*^{Mrp8cre} mice after colonisation with *C. albicans*. Data are mean±SEM of two independent experiments. *p<0.05, **p<0.01, ***p<0.001, ****p<0.0001 as determined by one-way ANOVA with Tukey's post-test (A), two-way ANOVA with Sidak's post-test (E, F) and Mann-Whitney test (C, G, I–K). Genta, gentamycin. ANOVA, analysis of variance; DSS, dextran sulfate sodium.

The absence of *Card9* impacts neutrophils survival by increasing apoptosis

To explore the mechanisms underlying the impaired capacity of *Card9*^{Mrp8cre} neutrophils to kill *C. albicans* despite intact phagocytosis, autophagy and ROS production, we investigated neutrophils survival rates by flow cytometry using an AnnexinV-FITC assay coupled to Live/Dead staining (figure 5). AnnexinV reveals ongoing apoptosis, whereas live/dead only stains permeable dead cells. Interestingly, after 1-hour incubation at 37°C, *Card9*^{Mrp8cre} neutrophils showed a significant increase in AnnexinV-FITC MFI compared with *Card9*^{Mrp8wt} neutrophils (figure 5A,B). Consistently, an increase in percentages of apoptotic (Q1, AnnexinV$^+$LD$^-$) and dead (late apoptotic/necrotic) neutrophils (Q2, AnnexinV$^+$LD$^+$), and a decrease in viable neutrophils (Q4, AnnexinVLD$^-$), were observed for the *Card9*^{Mrp8cre} genotype (figure 5C). Moreover, the surface expression of the CD62L marker (a surface protein that is lost on cell activation) was reduced in *Card9*^{Mrp8cre}, with a lower percentage of CD62L$^+$ cells and a higher percentage of CD62L$^-$ cells (figure 5D). These results suggest an excessive basal activation of *Card9*^{Mrp8cre} compared with *Card9*^{Mrp8wt} neutrophils. Similar results were obtained with *Card9*$^{-/-}$ versus Card9WT neutrophils (online supplemental figure S5A–D), confirming the impact of *Card9* on neutrophil survival.

To go further, we performed a proteomic analysis on *Card9*^{Mrp8cre} vs *Card9*^{Mrp8wt} neutrophils after 1-hour incubation at 37°C. This approach revealed that a large number of proteins related to cellular metabolism pathways were differentially regulated between both genotypes. Indeed, a gene ontology (GO) functional analysis showed the enrichment in numerous cellular metabolic processes among proteins statistically downregulated or upregulated in *Card9*^{Mrp8cre} compared with *Card9*^{Mrp8wt} neutrophils (figure 5E and online supplemental figure S5E). Especially, we observed a high prevalence of mitochondrial

Gut: first published as 10.1136/gutjnl-2022-326917 on 27 September 2022. Downloaded from http://gut.bmj.com/ on October 9, 2024 at Library of Vilnius University. Protected by copyright.

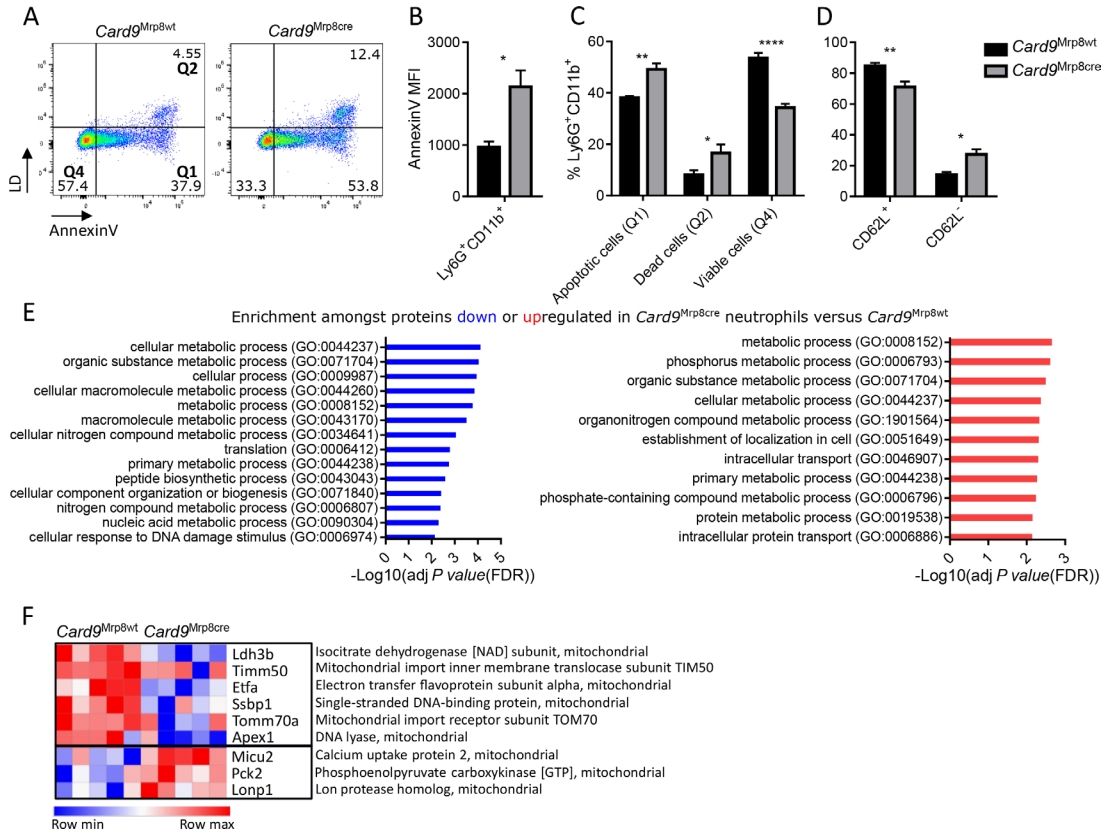

Figure 5 The absence of *Card9* impacts neutrophils survival by increasing apoptosis. (A) Representative flow cytometry plots of Ly6G$^+$CD11b$^+$ neutrophils purified from bone marrow of *Card9*^{Mrp8wt} (left) and *Card9*^{Mrp8cre} (right) mice, co-stained with AnnexinV and a Live/Dead marker. (B) AnnexinV MFI of Ly6G$^+$CD11b$^+$ neutrophils from *Card9*^{Mrp8wt} and *Card9*^{Mrp8cre} mice, incubated for 1 hour at 37°C. (C) Percentage of apoptotic neutrophils (Q1: AnnexinV$^+$LD$^-$ cells), dead (late apoptotic/necrotic) neutrophils (Q2: AnnexinV$^+$LD$^+$ cells) and viable neutrophils (Q4: AnnexinV$^-$LD$^-$ cells) among the Ly6G$^+$CD11b$^+$ population. (D) Percentage of CD62L$^+$ and CD62L$^-$ neutrophils among the Ly6G$^+$CD11b$^+$ population. Data represent one out of two independent experiments. (E) Histogram representing Gene Ontology biological processes significantly enriched among proteins downregulated (blue) or upregulated (red) in *Card9*^{Mrp8cre} compared with *Card9*^{Mrp8wt} neutrophils in the unstimulated condition. (F) Morpheus heatmap representing mitochondria-related proteins significantly downregulated or upregulated in *Card9*^{Mrp8cre} compared with *Card9*^{Mrp8wt} neutrophils in the unstimulated condition. (E, F) Obtained from proteomics data analysis. *p<0.05, **p<0.01, ****p<0.0001 as determined by Mann-Whitney U test (B) and two-way ANOVA with Sidak's post-test (C–D). ANOVA, analysis of variance; MFI, mean fluorescence intensity.

proteins among the differentially regulated candidates between the two genotypes (figure 5F), suggesting that neutrophil mitochondrial functions are impacted by the absence of *Card9*.

Card9 controls neutrophil survival by affecting mitochondrial function

Subsequently, we analysed neutrophil mitochondrial function using MitoTracker Green (reflecting mitochondrial mass) and MitoTracker Red (reflecting mitochondrial membrane potential) markers in a flow cytometry assay (figure 6A). No difference was observed in terms of MFIs, but we observed a significant increase in the percentage of MitoGreen$^+$MitoRed$^-$ neutrophils (with dysfunctional or metabolically inactive mitochondria) in the *Card9*^{Mrp8cre} compared with the *Card9*^{Mrp8wt} genotype (figure 6A). Tetramethylrhodamine methyl ester (TMRM) assay evaluating the mitochondrial membrane potential confirmed the increase in apoptotic, metabolically stressed cells (TMRM$^-$) among *Card9*^{Mrp8cre} neutrophils (figure 6B). These results suggest that the survival defect of *Card9*^{Mrp8cre} neutrophils may be due to an altered energetic metabolism. Real-time bioenergetic profile analysis using Seahorse technology showed that *Card9*^{Mrp8cre} neutrophils have a higher basal Oxygen Consumption Rate during a cell mito stress assay (figure 6C), indicating a higher oxidative phosphorylation activity compared with *Card9*^{Mrp8wt} neutrophils. Basal respiration and ATP production rate were both highly increased in *Card9*^{Mrp8cre} neutrophils (figure 6D). Moreover, a Seahorse real-time ATP rate assay demonstrated that *Card9*^{Mrp8cre} neutrophils have an increased mitochondrial ATP (mitoATP) production rate, whereas glycolytic ATP (glycoATP) production rate is only mildly decreased, as shown by the ATP rate index and the energetic map (figure 6E). A Seahorse glycolytic rate assay confirmed the moderate decrease of the basal Extracellular Acidification Rate of *Card9*^{Mrp8cre} neutrophils (online supplemental figure S6A). However, metabolomics analysis on neutrophil supernatants incubated for 24 hours revealed a decreased in lactate production, leading to a reduced lactate/glucose ratio in *Card9*^{Mrp8cre} neutrophils (online supplemental figure S6B). Similar results were obtained when we compared Card9WT and *Card9*$^{-/-}$ neutrophils in the assays described above (online supplemental figure S6C–E). Thus, *Card9* deletion in neutrophils induces an overactivation of mitochondria and tends to reduce glycolytic activity, which is the major energy source of normal neutrophils. Blocking glycolysis with 2DG (2-Deoxy-D-glucose) increased the apoptotic rate of *Card9*^{Mrp8wt} but not of *Card9*^{Mrp8cre} neutrophils; showing that glycolysis is more essential to *Card9*^{Mrp8wt} than *Card9*^{Mrp8cre} neutrophils

Gut: first published as 10.1136/gutjnl-2022-326917 on 27 September 2022. Downloaded from http://gut.bmj.com/ on October 9, 2024 at Library of Vilnius University. Protected by copyright.

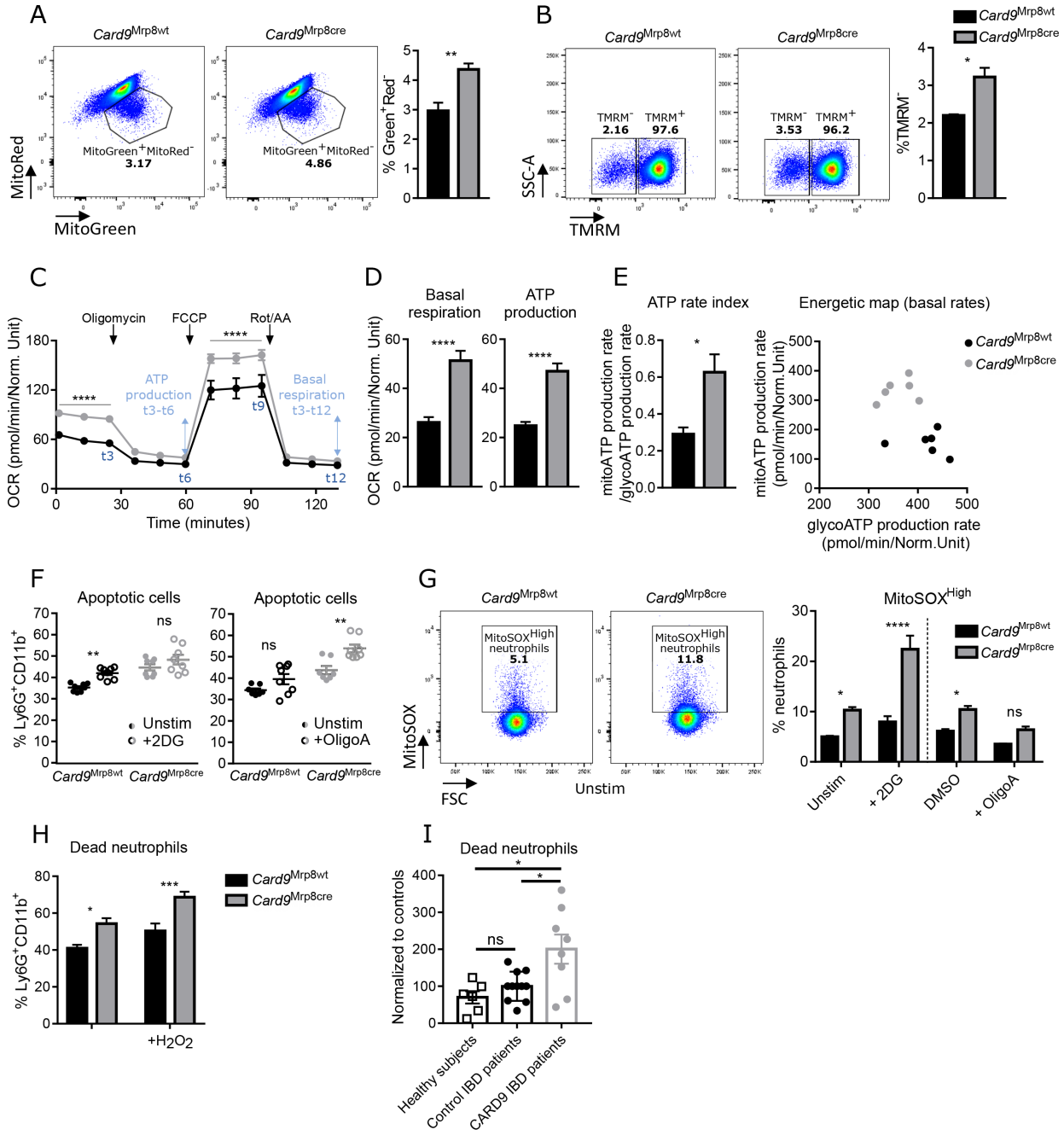

Figure 6 *Card9* controls neutrophil energetic metabolism by affecting mitochondrial function. (A) Representative flow cytometry plots and precentages of MitoGreen^{+}MitoRed^{-} cells (corresponding to cells with dysfunctional mitochondria) among Ly6G^{+}CD11b^{+} neutrophils. Neutrophils were purified from the bone marrow of *Card9*^{Mrp8wt} or *Card9*^{Mrp8cre} mice, and incubated for 1 hour at 37°C. (B) Representative flow cytometry plots and percentages of TMRM^{-} cells (corresponding to cells with dysfunctional mitochondria/apoptotic or metabolically inactive cells) among Ly6G^{+}CD11b^{+} neutrophils. (C) Oxygen consumption rate (OCR) of *Card9*^{Mrp8wt} and *Card9*^{Mrp8cre} neutrophils measured during a Seahorse Cell Mito Stress assay. (D) Basal respiration (late rate measurement before oligomycin injection (t3) - non-mitochondrial respiration rate (t12)) and ATP production rate (late rate measurement before oligomycin (ATP synthase blocker) injection (t3) – minimum rate measurement after oligomycin injection (t6) obtained from the Seahorse Cell Mito Stress assay. (E) ATP rate index and energetic map of *Card9*^{Mrp8wt} and *Card9*^{Mrp8cre} neutrophils obtained from the Seahorse Real-time ATP rate assay. (F) Percentage of apoptotic cells among the Ly6G^{+}CD11b^{+} neutrophil population of *Card9*^{Mrp8wt} and *Card9*^{Mrp8cre} genotypes after treatment with 2-DG 10 mM (left) or oligomycin 1.5 µM (right) for 1 hour. (G) Representative flow cytometry plots and precentages of MitoSOX^{high} cells (corresponding to cells with high mitochondrial ROS) among *Card9*^{Mrp8wt} and *Card9*^{Mrp8cre} neutrophils incubated for 1 hour at 37°C. (H) Percentage of apoptotic and necrotic cells among the Ly6G^{+}CD11b^{+} neutrophil population of *Card9*^{Mrp8wt} and *Card9*^{Mrp8cre} genotypes after addition of H2O2 0.01 mM for 1 hour to increase oxydative stress. (I) Death rate of human blood neutrophils from patients with IBD carrying the CARD9 single-nucleotide polymorphism most commonly associated with IBD (rs10781499, homozygous state, n=8) and age-matched and sex-matched control patients with IBD (n=11) and healthy subjects (n=6). Data are mean±SEM of at least two independent experiments. *p<0.05, **p<0.01, ***p<0.001, ****p<0.0001 as determined by Mann-Whitney test (A, B, D, E, I) or two-way ANOVA with Sidak's post-test (F, G, H). Norm. Unit, normalised unit; FCCP, Carbonyl cyanide 4-(trifluoromethoxy)phenylhydrazone; Rot/AA, Rotenone/AntimycinA; 2DG, 2 deoxy-glucose; OligoA, oligomycinA. ANOVA, analysis of variance; IBD, inflammatory bowel disease; ROS, reactive oxygen species.

Gut: first published as 10.1136/gutjnl-2022-326917 on 27 September 2022. Downloaded from http://gut.bmj.com/ on October 9, 2024 at Library of Vilnius University. Protected by copyright.

(figure 6F, left). Conversely, blocking the mitochondrial respiratory chain with oligomycineA increased the apoptotic rate of *Card9*^{Mrp8cre} but not of *Card9*^{Mrp8wt} neutrophils, demonstrating the crucial role of mitochondria as an energy source in *Card9*^{Mrp8cre} neutrophils (figure 6F, right). Thus, contrary to *Card9*^{Mrp8wt} neutrophils that mainly rely on glycolysis as a source of energy, *Card9*^{Mrp8cre} neutrophils present an altered metabolism with an overactivation of mitochondria associated with a dysfunctional state, leading to apoptosis. Indeed, we showed by MitoSOX staining that the production of mitochondrial ROS (mtROS) is increased in *Card9*^{Mrp8cre} compared with *Card9*^{Mrp8wt} neutrophils (figure 6G, left). This difference is increased by 2-DG treatment as mitochondrial respiration is promoted (figure 6G, right). Conversely, blocking mitochondrial respiration with oligomycinA decreases the differences between *Card9*^{Mrp8cre} and *Card9*^{Mrp8wt} neutrophils (figure 6G, right). These results show that the increased mitochondrial respiration in *Card9*^{Mrp8cre} neutrophils generates increased mtROS production, major determinant of cell apoptosis.[31] Intestinal inflammation is associated with a high degree of oxidative stress. To evaluate the effect of oxidative stress on the phenotype of *Card9*^{Mrp8cre} neutrophils, they were treated for 1 hour with H_2O_2. The increased apoptosis and necrosis rates observed in *Card9*^{Mrp8cre} neutrophils were stronger in oxidative stress than in basal condition (figure 6H). These results show that the role of CARD9 in the survival capacity of neutrophils, especially in oxidative conditions, is mediated by effects on mitochondrial functions. Consistently, blood neutrophils from patients with IBD carrying the CARD9 single-nucleotide polymorphism most commonly associated with IBD (rs10781499, homozygous state) had an increased mortality rate compared with age-matched and sex-matched control patients with IBD and healthy subjects (figure 6I).

DISCUSSION

Altogether, this study reveals that, in the absence of CARD9, mitochondrial dysfunction in neutrophils leads to their premature death through apoptosis, especially in an oxidative environment. The decrease of functional neutrophils in the gut affects fungal containment and increases susceptibility to intestinal inflammation. CARD9 polymorphisms are associated with IBD. Mouse studies showed the contribution of CARD9 to host defence and intestinal barrier, notably through the production of IL-22 and the modulation of the gut microbiota metabolic activity.[25 26] However, the role of CARD9 in disease pathogenesis has not been elucidated at the cellular level. Our study reveals that *Card9* deletion in neutrophils, contrarily to epithelial or CD11c$^+$ cells, increases the susceptibility to DSS-induced colitis. We thus focused on studying the role of CARD9 expression in neutrophil functionality. Indeed, neutrophils have been studied in different models of IBD and fungal infection, but their direct contribution to pathogenesis and the role of CARD9 in these mechanisms remain poorly understood.[4 5 32 33]

Human CARD9 deficiency results in impaired neutrophil fungal killing, leading to a selective defect to contain invasive fungal infection.[34] In both humans and mice, CARD9 is required in microglia for neutrophil recruitment and control of fungal infection in the central nervous system.[35 36] CARD9 signalling was also involved in neutrophil phagocytosis and NETosis (neutrophil extracellular traps) functions, enhancing mouse survival to a lethal dose of *C. albicans*.[37] Moreover, CARD9 expression in neutrophils promotes autoantibody-induced arthritis and dermatitis in mice,[38] and inflammation levels in a mouse model of neutrophilic dermatosis.[39] In line with these studies, we found that *Card9* deletion affects the capacity of neutrophils to kill fungi in vitro and in vivo, but we found no impact on the neutrophil structure, ROS production, autophagy, phagocytosis or NETosis. We have not examined the role of CARD9 in chemotaxis because, in the context of fungal infection in patients with CARD9 deficiency, neutrophil-intrinsic chemotaxis was not affected.[24] In DSS-induced colitis, *Card9* deficiency in neutrophils does not impact their recruitment to the colon, but reduces the number of mature neutrophils. We do not think that impaired antimycotic function explains the increased susceptibility to colitis but rather reveals that CARD9-deficient neutrophils have a major functional defect. Indeed, we discovered that the absence of CARD9 increases mortality in both mouse and human neutrophils. This premature death is caused by mitochondria overactivation and the increased production of mtROS. Indeed, mtROS are generated as byproducts of mitochondrial respiration and are major determinants of cell apoptosis.[31] Other CARD proteins mediate apoptotic signalling through CARD-CARD domain interactions.[13] In addition to mediating inflammation, CARD9, a member of the CARD proteins family, was recently shown to inhibit mitochondria-dependent apoptosis of cardiomyocytes under oxidative stress.[40] Here, we show that CARD9 mediates mitochondrial function and apoptosis in neutrophils, especially in an oxidative environment. Interestingly, mitochondrial dysfunction was observed in human in the context of active UC.[41] Further investigation is required to fully elucidate the impact of mitochondria overactivation on neutrophil function, especially in vivo. The impact of *Card9* on neutrophil mitochondrial function might not fully explain the increased susceptibility of *Card9*^{Mrp8cre} mice to DSS colitis. Moreover, other cell types are likely involved in the *Card9*$^{-/-}$ mice phenotype, explaining the impact of *Card9* deletion on microbiota metabolic activity, as we show that this is not dependent on neutrophils.[25 26]

Neutrophils contain very few mitochondria compared with other leukocytes, and depend mainly on glycolysis to produce ATP, which is essential to perform their designated tasks. This allows energy generation in a low-oxygen environment and keeps oxygen available for neutrophil effector functions.[42] Thus, the dependence of neutrophils on glycolysis could be an adaptation to allow oxygen to be used in the anti-microbial response rather than entering oxidative phosphorylation.[42] Here, we show that in the absence of CARD9, mitochondria overactivation, leads to the premature death of neutrophils through apoptosis and the loss of their anti-microbial functions. DSS and anti-CD40 colitis models performed with the addition of anti-Ly6G antibody, which specifically depletes neutrophils, show that the absence of neutrophils strongly exacerbates gut inflammation and impacts mouse survival.[43] In humans, neutropenia is associated with severe intestinal inflammation, in the case of neutropenic enterocolitis[44] and IBD-like phenotype in phenotype in patients with CGD[45] for instance. Excessive oxidative phosphorylation and mitochondrial ATP production in neutrophils can also damage the surrounding tissues and exacerbate inflammation. This could explain the increased susceptibility to intestinal colitis in the absence of *Card9*, especially in inflammatory environments where neutrophil activity is normally tightly controlled by the low oxygen pressure. In humans, the « glycogen storage disease type Ib » induces a functional defect of neutrophils due to glycolysis dysfunction and impaired energy homeostasis.[46] This disease is associated with IBD-like phenotypes, highlighting the importance of neutrophil metabolism in intestinal health.[46 47] Immunometabolism is a central concept as immunity and metabolism impact each other in both ways: (1)

Gut: first published as 10.1136/gutjnl-2022-326917 on 27 September 2022. Downloaded from http://gut.bmj.com/ on October 9, 2024 at Library of Vilnius University. Protected by copyright.

energetic metabolism impacts immune function, which is well documented for lymphocytes and macrophages,[48] but not for neutrophils; and (2) we show that a protein known for its roles in innate immunity, CARD9, can also impact cell metabolism. Further investigation is required to understand how CARD9 does interact with mitochondrial function in a direct or indirect manner.

Neutrophils are involved in various diseases, including infection, cardiovascular diseases, inflammatory disorders and cancer, which makes them exciting targets for therapeutic intervention.[49] Despite the complex implication of neutrophils in disease, various therapeutic approaches aim to enhance, inhibit or restore neutrophil function, depending on the pathology. In inflammatory diseases with excessive neutrophil activity, their attenuation could be desired, even though killing functions against microorganisms might still need to be preserved. Our work shows that increased apoptosis in neutrophils does not alleviate intestinal inflammation, even though these cells are known to contribute to disease development. Recent studies indicate substantial phenotypic and functional heterogeneity of neutrophils.[49] Thus, targeting a specific subpopulation may allow the attenuation of harmful aspects of neutrophils without compromising host defence. Some neutrophil-targeted therapeutic strategies have gained interest, notably in the context of IBD with positive effects of the growth factor granulocyte colony-stimulating factor (G-CSF).[50] Recently, anti-GM-CSF autoantibodies have also been shown to precede Crohn's disease onset by years.[51] It opens promising options for numerous complex pathologies.

MATERIAL AND METHODS

Mice

Card9$^{-/-}$, *Rag2*$^{-/-}$x*Card9*$^{-/-}$, *Rag2*$^{-/-}$, *Card9*loxxMrp8cre, *Card9*loxxVillincre and *Card9*loxxCD11ccre mice on C57BL/6J background were obtained from the Saint-Antoine Research Centre and housed at the IERP (INRAE, Jouy-en-Josas) under specific pathogen-free conditions. Animal experiments were performed according to the institutional guidelines approved by the local ethics committee of the French authorities, the 'Comité d'Ethique en Experimentation Animale' (COMETHEA, CEEA45).

Induction of DSS colitis and colonisation with *C. albicans*

Mice were administered drinking water supplemented with 2–3% (wt/vol) DSS (MP Biomedicals) for 5–7 days (depending on colitis severity of each experiment), and then water only for 5 days. Animals were monitored daily for weight loss. For *C. albicans* colonisation, mice were treated with 0.4 mg/mL streptomycin, 300 U/mL penicillin G and 0.125 mg/mL fluconazole as indicated in figure 4.

Histology

Colon samples were fixed, embedded in paraffin and stained with H&E. Slides were scanned and analysed to determine the histological score (online supplemental table S1).[25]

Faecal DNA extraction and total bacteria and fungi quantification

Faecal DNA was extracted as previously described.[26] Luna Universal qPCR Master Mix (New England Biolabs) was used for quantification of fungal ITS2 sequences and TaqMan Gene Expression Assays (Life Technologies) for quantification of bacterial 16S rDNA sequences.

Cell preparation and stimulation

Epithelial cells were isolated from colonic tissue using a dithiothreitol (DTT)/ethylenediaminetetraacetic (EDTA) buffer. Neutrophils were purified from mouse bone marrow using anti-Ly6G MicroBeads UltraPure and MACS separation columns (Miltenyi Biotec). CD11c^{+} cells were purified from mouse spleen using anti-CD11c MicroBeads UltraPure and MACS separation columns (Miltenyi Biotec). Purity checks and cell counts were performed using a BD Accuri C6 flow cytometer (BD Biosciences). After purification, neutrophils were seeded in 96-well suspension plate (Sarstedt), rested for 30 min in RPMI 1640 Medium (Gibco, ThermoFisher Scientific) before addition of 2% heat-inactivated Fetal Bovine Serum (FBS), 2-DG 10 mM, oligomycine 1.5μM or H2O2 0.01M and incubated at 37°C as indicated. Isolation of LP immune cells was performed as previously described.[52]

Gene expression analysis using quantitative RT-PCR

Total RNA was isolated from colon samples or cell suspensions using RNeasy Mini Kit (Qiagen), and quantitative RT-PCR performed using QuantiTect Reverse Transcription Kit (Qiagen) and Luna Universal RT-PCR Kit (New England Biolabs) in a StepOnePlus apparatus (Applied Biosystems) with specific mouse oligonucleotides (online supplemental table S2). We used the $2-\Delta\Delta^{Ct}$ quantification method with mouse *Gapdh* as an endogenous control and the WT group as a calibrator.

Immunoblot Analysis. Mouse tissue or cell suspensions were lysed using Laemmli buffer, loaded on a SDS-PAGE and analysed with antibodies against CARD9 (A-8:sc-374569, Santa Cruz Biotechnology), or β-ACTIN (D6A8, CST).

Flow cytometry, cell sorting and functional assays

Flow cytometry was carried out by using LSR Fortessa X-20 (BD) and cell sorting FACS Aria machines (BD). For apoptosis assay, 4×10^{5} neutrophils were stained with AnnexinV-FITC in Binding Buffer (Miltenyi Biotec) and Live/Dead (Zombie Aqua Fixable, BioLegend). For mitochondria analyses, MitoTracker Green and MitoTracker Red FM or MitoSOX Red Mitochondrial Superoxide Indicator, were added to neutrophils for 15 min at RT in MACS buffer or PBS, respectively (ThermoFisher Scientific). Alternatively, neutrophils were incubated with TMRM in RPMI for 20 min at 37°C (Abcam). For phagocytosis assay, 10^{5} neutrophils stimulated with zymosan-FITC (50μg/ml, Fluorescein zymosanA BioParticles conjugates, FisherScientific), *C. albicans*-GFP (MOI1:1) or *Escherichia coli*-GFP (MOI1:10) for 45 min. Cells were stained with surface antibodies in MACS buffer (online supplemental table S2).

Endpoint dilution survival assay

Isolated mouse neutrophils were seeded at 10^{5} cells/well in 96-well plates in RPMI+2% FBS and infected with *C. albicans* (serial fourfold dilutions of an OD=1 solution were added by raws (row1, MOI20:1; row2, MOI5:1…). After 24 hours at 37°C, colonies were visualised with a Nikon TMS inverted microscope and counted at the lowest dilutions (row7-8).

Killing assay

Purified neutrophils were seeded in 96-well plate at 10^{6} cells/well and stimulated with PBS, *C. albicans* (MOI1) or *E. coli* (MOI10) for 90 min at 37°C. Cells were washed and lysed with 200μl TritonX100 0.025%. Serial dilutions were plated on YEPD or LB plates.

Gut: first published as 10.1136/gutjnl-2022-326917 on 27 September 2022. Downloaded from http://gut.bmj.com/ on October 9, 2024 at Library of Vilnius University. Protected by copyright.

Oxydative burst

Experiments were performed on a TriStar LB942 Reader using 10^5 neutrophils in 200 µL Hank's Balanced Salt Solution (HBSS, ThermoFisher Scientific) and luminol 80μM (Sigma) and stimulated with PMA (0.1 µg/mL; Sigma) or opsonised zymosan (20 mg/mL zymosan A from *Saccharomyces cerevisiae*; Sigma). The indexed maximal relative luminescence (in relative light units (RLU)) was calculated as follow: indexed RLU max=((haemochromatosis patient maximal RLU)/(healthy donor maximal RLU))×100. Alternatively, superoxyde dismutase (5 units/mL) and catalase A (10Units/mL) were added to differentiate total and intracellular ROS production. Absorbance was measured at 550 nm for 30 min.

Real time bioenergetic profile analysis

Mito Stress Test, Glycolytic Rate Assay and Real-time ATP assay were performed on a XF96 Extracellular Flux Analyzer (Seahorse Biosciences). Mouse neutrophils were seeded at 2×10^5 cells/well in RPMI+2%FBS in 0.01% poly-L-lysine precoated plate. After 2-hour rest, cells were washed in Seahorse RPMI medium and incubated for 1 hour at 37°C without CO2. In the analyzer, oligomycin 1.5 µM, FCCP 1 µM, rotenone+antimycinA 0.5 µM and 2DG 50 µM were injected at the indicated times. Protein standardisation was performed after each experiment, with no noticeable differences in protein concentration and cell phenotype.

Electron microscopy

Purified neutrophils were stimulated with *C. albicans* (MOI 2) or *E. coli* (MOI 10) for 1 hour at 37°C, washed in PBS and fixed. Samples preparation and SEM/TEM analyses were performed at the Microscopy and Imaging Platform MIMA2 (Université Paris-Saclay, INRAE, AgroParisTech, Jouy-en-Josas, France, https://doi.org/10.15454/1.5572348210007727E12).

Proteomics

The 5 µg protein extracts were submitted to in-gel digestion. Desalting was performed as described before.[53] Peptides were analysed on a nanoElute-timsTOF ProLC-MS/MS system (Bruker).[54] Raw files were analysed using MaxQuant V.1.6.10.43: database UP000000589_10090 (21 994 entries, 17 June 2020). Data filtering, imputation and statistical analysis were performed with ProStar Zero V.1.20.0.[54] Proteins with False Discovery Rate (FDR <5% (Pounds method) were significant with a fold change >1.2.

Nuclear magnetic resonance

The 200 µL culture media were analysed by 1D 1H-NMR. All NMR spectra were recorded on a Bruker AvanceIII 800MHz spectrometer equipped with a QPCI 5 mm cryogenic probe head. Spectra were acquired and processed using the Bruker Topspin V.4.0 software. Quantification of glucose and lactate was performed using addition of 25% TSPd4 in D2O as internal standard.

Patients and samples collection

A diagnosis of IBD was defined by clinical, radiological, endoscopic and histological criteria. Patient characteristics are presented in online supplemental table S3. Human blood neutrohpils were isolated using the technique of dextran sedimentation and Ficoll density gradient, and stained with AnnexinV-FITC (Miltenyi Biotec) and a Live/Dead marker (Zombie Aqua Fixable, BioLegend). Data were acquired using a CytoFlex cytometer (Beckman).

Statistical analysis

Statistical analysis was performed using GraphPad Prism V.7 software.

Author affiliations
[1]Université Paris-Saclay, INRAE, AgroParisTech, Micalis Institute, Jouy-en-Josas, France
[2]Sorbonne Université, INSERM UMRS-938, Centre de Recherche Saint-Antoine, CRSA, AP-HP, Hôpital Saint-Antoine, Service de Gastroentérologie, F-75012 Paris, France
[3]Paris Center For Microbiome Medicine (PaCeMM) FHU, Paris, France
[4]CNRS, UPR 9002, Université de Strasbourg, Institut de Biologie Moléculaire et Cellulaire, Architecture et Réactivité de l'ARN, Strasbourg, France
[5]Sorbonne Université, INSERM, UMS PASS, Plateforme Postgénomique de la Pitié Salpêtrière (P3S), Paris, France
[6]MetaToul-MetaboHUB, National Infrastructure of Metabolomics & Fluxomics (ANR-11INBS-0010), 31077 Toulouse, France
[7]Aix Marseille Univ, CNRS, INSERM, CIML, Centre d'Immunologie de Marseille-Luminy, Marseille, France
[8]Institut Cochin, INSERM, CNRS, Université de Paris, Laboratoire d'excellence GR-Ex, Paris, France
[9]Université de Paris, INSERM-U1149, CNRS-ERL8252, Centre de Recherche sur l'Inflammation (CRI), Laboratoire d'excellence Inflamex, Faculté de Médecine Xavier Bichat, Paris, France
[10]University of Strasbourg Institute for Advanced Study (USIAS), Strasbourg, France
[11]Institut Pasteur, Université de Paris, Inserm 1225 Unité de Pathogenèse des Infections Vasculaires, 28 rue du Dr. Roux, 75724 Paris Cedex 15, France

Twitter Harry Sokol @h_sokol

Contributors CD and HS conceived and designed the study, performed data analysis and wrote the manuscript and both act as guarantor; CD designed and conducted all experiments, unless otherwise indicated; CM, JP, AM, AA, M-LM, BL, GDC, MS, CG, MP, YW and AL provided technical help for the in vitro and/or in vivo experiments; JS and BM performed the immunofluorescence microscopy experiments; CéP and SC conducted the proteomics analyses; FB, EC and AR performed the metobolomics analysis; TL provided mice and CO performed genotyping; CaP, SL and JE-B helped with ROS production assays; RRA provided Scenith kits for tests with neutrophils; CD, CM, JP, MLR, PL, NR, JE-B, BM and HS discussed experiments and results.

Competing interests None declared.

Patient and public involvement Patients and/or the public were involved in the design, or conduct, or reporting, or dissemination plans of this research. Refer to the Methods section for further details.

Patient consent for publication Not applicable.

Ethics approval Approval was obtained from the local ethics committee (Comite de Protection des Personnes Ile-de-France IV, IRB 00003835, Suivitheque study, registration number 2012/05NICB). Participants gave informed consent to participate in the study before taking part.

Provenance and peer review Not commissioned; externally peer reviewed.

Data availability statement All data relevant to the study are included in the article or uploaded as online supplemental information.

Supplemental material This content has been supplied by the author(s). It has not been vetted by BMJ Publishing Group Limited (BMJ) and may not have been peer-reviewed. Any opinions or recommendations discussed are solely those of the author(s) and are not endorsed by BMJ. BMJ disclaims all liability and responsibility arising from any reliance placed on the content. Where the content includes any translated material, BMJ does not warrant the accuracy and reliability of the translations (including but not limited to local regulations, clinical guidelines, terminology, drug names and drug dosages), and is not responsible for any error and/or omissions arising from translation and adaptation or otherwise.

Open access This is an open access article distributed in accordance with the Creative Commons Attribution 4.0 Unported (CC BY 4.0) license, which permits others to copy, redistribute, remix, transform and build upon this work for any purpose, provided the original work is properly cited, a link to the licence is given, and indication of whether changes were made. See: https://creativecommons.org/licenses/by/4.0/.

ORCID iD
Camille Danne http://orcid.org/0000-0003-0971-8310

Gut: first published as 10.1136/gutjnl-2022-326917 on 27 September 2022. Downloaded from http://gut.bmj.com/ on October 9, 2024 at Library of Vilnius University. Protected by copyright.

REFERENCES

1 Plichta DR, Graham DB, Subramanian S, *et al*. Therapeutic opportunities in inflammatory bowel disease: mechanistic dissection of host-microbiome relationships. *Cell* 2019;178:1041–56.
2 Graham DB, Xavier RJ. Pathway paradigms revealed from the genetics of inflammatory bowel disease. *Nature* 2020;578:527–39.
3 Dave M, Papadakis KA, Faubion WA. Immunology of inflammatory bowel disease and molecular targets for biologics. *Gastroenterol Clin North Am* 2014;43:405–24.
4 Wéra O, Lancellotti P, Oury C. The dual role of neutrophils in inflammatory bowel diseases. *J Clin Med* 2016;5:118.
5 Zhou GX, Liu ZJ. Potential roles of neutrophils in regulating intestinal mucosal inflammation of inflammatory bowel disease. *J Dig Dis* 2017;18:495–503.
6 Caër C, Wick MJ. Human intestinal mononuclear phagocytes in health and inflammatory bowel disease. *Front Immunol* 2020;11:410.
7 Kolaczkowska E, Kubes P. Neutrophil recruitment and function in health and inflammation. *Nat Rev Immunol* 2013;13:159–75.
8 Segal AW. How neutrophils kill microbes. *Annu Rev Immunol* 2005;23:197–223.
9 Mulholland MW, Delaney JP, Foker JE, *et al*. Gastrointestinal complications of congenital immunodeficiency states. The surgeon's role. *Ann Surg* 1983;198:673–80.
10 Segal AW. The NADPH oxidase and chronic granulomatous disease. *Mol Med Today* 1996;2:129–35.
11 Annabi B, Hiraiwa H, Mansfield BC, *et al*. The gene for glycogen-storage disease type 1B maps to chromosome 11q23. *Am J Hum Genet* 1998;62:400–5.
12 Uzel G, Tng E, Rosenzweig SD, *et al*. Reversion mutations in patients with leukocyte adhesion deficiency type-1 (LAD-1). *Blood* 2008;111:209–18.
13 Bertin J, Guo Y, Wang L, *et al*. CARD9 is a novel caspase recruitment domain-containing protein that interacts with BCL10/CLAP and activates NF-kappa B. *J Biol Chem* 2000;275:41082–6.
14 Hsu Y-MS, Zhang Y, You Y, *et al*. The adaptor protein CARD9 is required for innate immune responses to intracellular pathogens. *Nat Immunol* 2007;8:198–205.
15 Zhernakova A, Festen EM, Franke L, *et al*. Genetic analysis of innate immunity in Crohn's disease and ulcerative colitis identifies two susceptibility loci harboring CARD9 and IL18RAP. *Am J Hum Genet* 2008;82:1202–10.
16 Franke A, McGovern DPB, Barrett JC, *et al*. Genome-wide meta-analysis increases to 71 the number of confirmed Crohn's disease susceptibility loci. *Nat Genet* 2010;42:1118–25.
17 Roth S, Ruland J. Caspase recruitment domain-containing protein 9 signaling in innate immunity and inflammation. *Trends Immunol* 2013;34:243–50.
18 McGovern DPB, Gardet A, Törkvist L, *et al*. Genome-wide association identifies multiple ulcerative colitis susceptibility loci. *Nat Genet* 2010;42:332–7.
19 Strasser D, Neumann K, Bergmann H, *et al*. Syk kinase-coupled C-type lectin receptors engage protein kinase C-δ to elicit CARD9 adaptor-mediated innate immunity. *Immunity* 2012;36:32–42.
20 Lanternier F, Mahdaviani SA, Barbati E, *et al*. Inherited CARD9 deficiency in otherwise healthy children and adults with Candida species-induced meningoencephalitis, colitis, or both. *J Allergy Clin Immunol* 2015;135:1558–68.
21 Cao Z, Conway KL, Heath RJ, *et al*. Ubiquitin ligase TRIM62 regulates CARD9-Mediated anti-fungal immunity and intestinal inflammation. *Immunity* 2015;43:715–26.
22 LeibundGut-Landmann S, Gross O, Robinson MJ, *et al*. Syk- and CARD9-dependent coupling of innate immunity to the induction of T helper cells that produce interleukin 17. *Nat Immunol* 2007;8:630–8.
23 Glocker E-O, Hennigs A, Nabavi M, *et al*. A homozygous *CARD9* mutation in a family with susceptibility to fungal infections. *N Engl J Med* 2009;361:1727–35.
24 Rieber N, Gazendam RP, Freeman AF. Extrapulmonary Aspergillus infection in patients with CARD9 deficiency JCI Insight; 2016: 1. https://insight.jci.org/articles/view/89890 [Accessed 15 Jun 2021].
25 Sokol H, Conway KL, Zhang M, *et al*. Card9 mediates intestinal epithelial cell restitution, T-helper 17 responses, and control of bacterial infection in mice. *Gastroenterology* 2013;145:591–601.
26 Lamas B, Richard ML, Leducq V, *et al*. CARD9 impacts colitis by altering gut microbiota metabolism of tryptophan into aryl hydrocarbon receptor ligands. *Nat Med* 2016;22:598–605.
27 Hartjes L, Ruland J. CARD9 signaling in intestinal immune homeostasis and oncogenesis. *Front Immunol* 2019;10:419.
28 Hara H, Ishihara C, Takeuchi A, *et al*. The adaptor protein CARD9 is essential for the activation of myeloid cells through ITAM-associated and Toll-like receptors. *Nat Immunol* 2007;8:619–29.
29 Bergmann H, Roth S, Pechloff K, *et al*. Card9-dependent IL-1β regulates IL-22 production from group 3 innate lymphoid cells and promotes colitis-associated cancer. *Eur J Immunol* 2017;47:1342–53.
30 Yang C-S, Rodgers M, Min C-K, *et al*. The autophagy regulator rubicon is a feedback inhibitor of CARD9-mediated host innate immunity. *Cell Host Microbe* 2012;11:277–89.
31 Silwal P, Kim JK, Kim YJ, *et al*. Mitochondrial reactive oxygen species: double-edged weapon in host defense and pathological inflammation during infection. *Front Immunol* 2020;11:1649.
32 Gazendam RP, van de Geer A, Roos D, *et al*. How neutrophils kill fungi. *Immunol Rev* 2016;273:299–311.
33 Desai JV, Lionakis MS. The role of neutrophils in host defense against invasive fungal infections. *Curr Clin Microbiol Rep* 2018;5:181–9.
34 Drewniak A, Gazendam RP, Tool ATJ, *et al*. Invasive fungal infection and impaired neutrophil killing in human CARD9 deficiency. *Blood* 2013;121:2385–92.
35 Drummond RA, Collar AL, Swamydas M, *et al*. CARD9-Dependent neutrophil recruitment protects against fungal invasion of the central nervous system. *PLoS Pathog* 2015;11:e1005293.
36 Drummond RA, Swamydas M, Oikonomou V, *et al*. CARD9^{+} microglia promote antifungal immunity via IL-1β- and CXCL1-mediated neutrophil recruitment. *Nat Immunol* 2019;20:559–70.
37 Loh JT, Xu S, Huo JX, *et al*. Dok3-protein phosphatase 1 interaction attenuates CARD9 signaling and neutrophil-dependent antifungal immunity. *J Clin Invest* 2019;129:2717–29.
38 Németh T, Futosi K, Sitaru C, *et al*. Neutrophil-Specific deletion of the CARD9 gene expression regulator suppresses autoantibody-induced inflammation in vivo. *Nat Commun* 2016;7:11004.
39 Tartey S, Gurung P, Samir P, *et al*. Cutting edge: dysregulated CARD9 signaling in neutrophils drives inflammation in a mouse model of neutrophilic dermatoses. *JI* 2018;201:1639–44.
40 Li Y, Liang P, Jiang B, *et al*. CARD9 inhibits mitochondria-dependent apoptosis of cardiomyocytes under oxidative stress via interacting with Apaf-1. *Free Radic Biol Med* 2019;141:172–81.
41 Haberman Y, Karns R, Dexheimer PJ, *et al*. Ulcerative colitis mucosal transcriptomes reveal mitochondriopathy and personalized mechanisms underlying disease severity and treatment response. *Nat Commun* 2019;10:38.
42 Burn GL, Foti A, Marsman G, *et al*. The neutrophil. *Immunity* 2021;54:1377–91.
43 Conway KL, Goel G, Sokol H, *et al*. P40Phox expression regulates neutrophil recruitment and function during the resolution phase of intestinal inflammation. *J Immunol* 2012;189:3631–40.
44 Rodrigues FG, Dasilva G, Wexner SD. Neutropenic enterocolitis. *World J Gastroenterol* 2017;23:42–7.
45 Yu H-H, Yang Y-H, Chiang B-L. Chronic granulomatous disease: a comprehensive review. *Clin Rev Allergy Immunol* 2021;61:101–13.
46 Jun HS, Weinstein DA, Lee YM, *et al*. Molecular mechanisms of neutrophil dysfunction in glycogen storage disease type Ib. *Blood* 2014;123:2843–53.
47 Yamaguchi T, Ihara K, Matsumoto T, *et al*. Inflammatory bowel disease-like colitis in glycogen storage disease type 1B. *Inflamm Bowel Dis* 2001;7:128–32.
48 Makowski L, Chaib M, Rathmell JC. Immunometabolism: from basic mechanisms to translation. *Immunol Rev* 2020;295:5–14.
49 Németh T, Sperandio M, Mócsai A. Neutrophils as emerging therapeutic targets. *Nat Rev Drug Discov* 2020;19:253–75.
50 Guidi L. Treatment of Crohn's disease with colony-stimulating factors: An overview. *TCRM* 2008;4:927–34.
51 Mortha A, Remark R, Del Valle DM. Neutralizing anti–granulocyte-macrophage–colony-stimulating factor autoantibodies recognize post-translational glycosylations on granulocyte-macrophage–colony-stimulating factor years before diagnosis and predict complicated Crohn's disease. *Gastroenterology* 2022:S0016508522005200.
52 Dupraz L, Magniez A, Rolhion N, *et al*. Gut microbiota-derived short-chain fatty acids regulate IL-17 production by mouse and human intestinal γδ T cells. *Cell Rep* 2021;36:109332.
53 Hamada S, Pionneau C, Parizot C, *et al*. In-depth proteomic analysis of *Plasmodium berghei* sporozoites using trapped ion mobility spectrometry with parallel accumulation-serial fragmentation. *Proteomics* 2021;21:2000305.
54 Pereira M, Richetta C, Sarango G. The autophagy receptor TAX1BP1 (T6BP) is a novel player in antigen presentation by MHC-II molecules. *Immunology* 2021.

Gut: first published as 10.1136/gutjnl-2022-326917 on 27 September 2022. Downloaded from http://gut.bmj.com/ on October 9, 2024 at Library of Vilnius University. Protected by copyright.

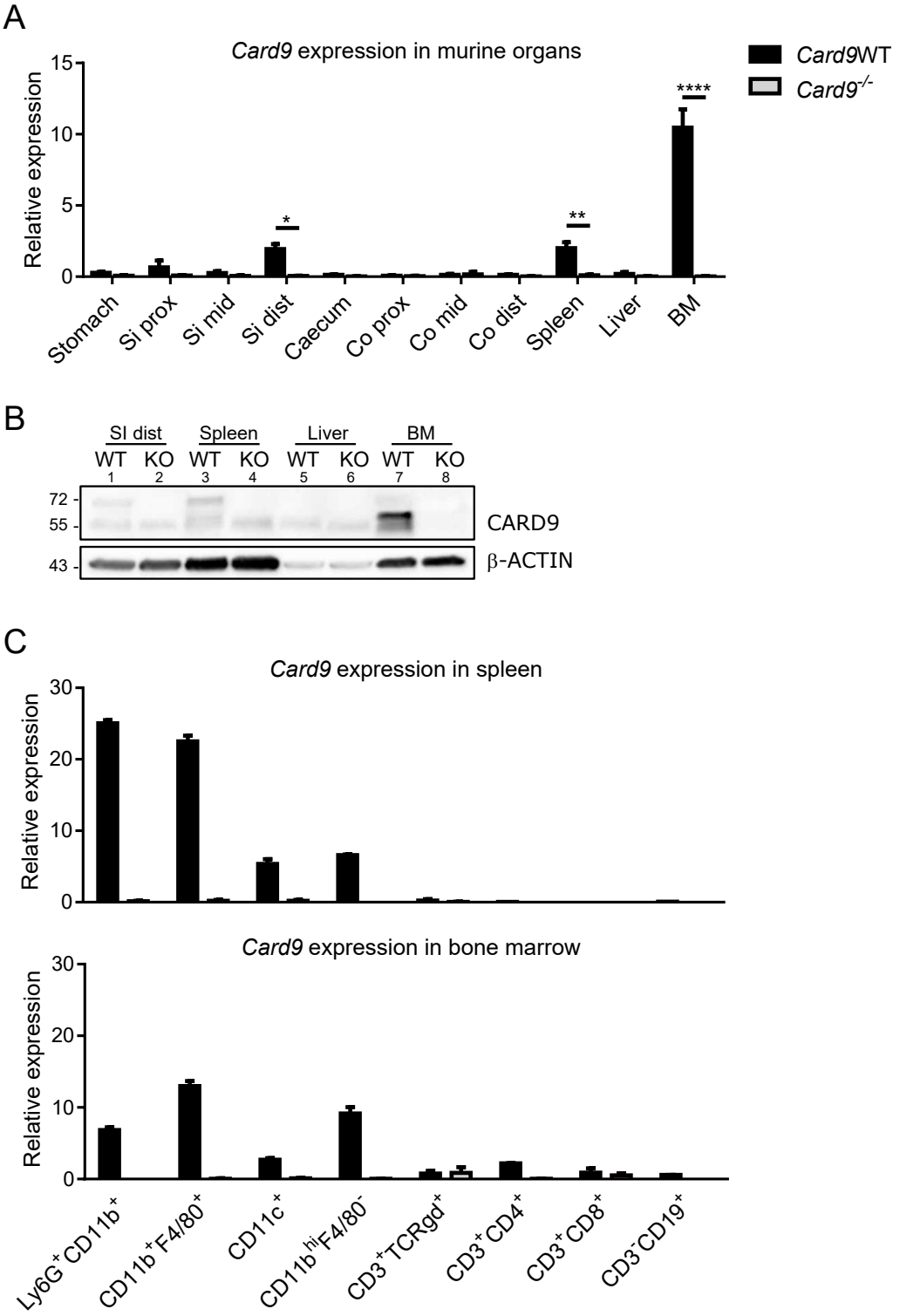
A
Card9 expression in murine organs
Card9WT
Card9-/-
Relative expression
15
10
5
0
*
**
****
Stomach
Si prox
Si mid
Si dist
Caecum
Co prox
Co mid
Co dist
Spleen
Liver
BM
B
SI dist
Spleen
Liver
BM
WT KO WT KO WT KO WT KO
1 2 3 4 5 6 7 8
72
55
43
CARD9
β-ACTIN
C
Card9 expression in spleen
Relative expression
30
20
10
0
Card9 expression in bone marrow
Relative expression
30
20
10
0
Ly6G+CD11b+
CD11b+F4/80+
CD11c+
CD11bhiF4/80-
CD3+TCRgd+
CD3+CD4+
CD3+CD8+
CD3-CD19+

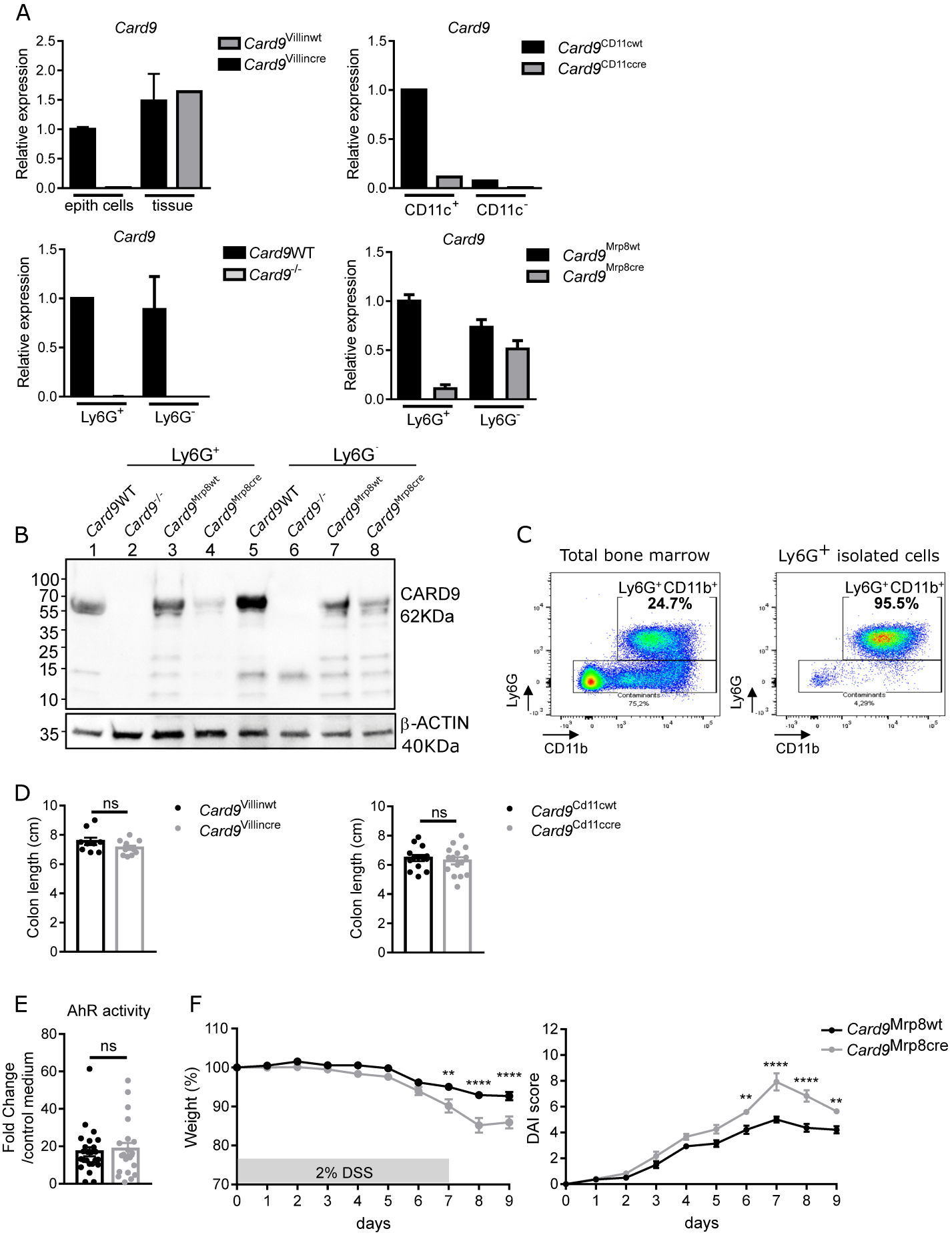
A
Card9
Relative expression
Card9Villinwt
Card9Villincre
epith cells
tissue
Card9
Card9CD11cwt
Card9CD11ccre
CD11c+
CD11c-
Card9
Card9WT
Card9-/-
Ly6G+
Ly6G-
Card9
Card9Mrp8wt
Card9Mrp8cre
B
Ly6G+
Ly6G-
Card9WT
Card9-/-
Card9Mrp8wt
Card9Mrp8cre
1 2 3 4 5 6 7 8
CARD9
62KDa
β-ACTIN
40KDa
C
Total bone marrow
Ly6G+ isolated cells
Ly6G+CD11b+
24.7%
95.5%
Ly6G
CD11b
Contaminants
75,2%
4,29%
D
Colon length (cm)
ns
Card9Villinwt
Card9Villincre
Card9Cd11cwt
Card9Cd11ccre
E
AhR activity
Fold Change /control medium
ns
F
Weight (%)
2% DSS
days
DAI score
Card9Mrp8wt
Card9Mrp8cre

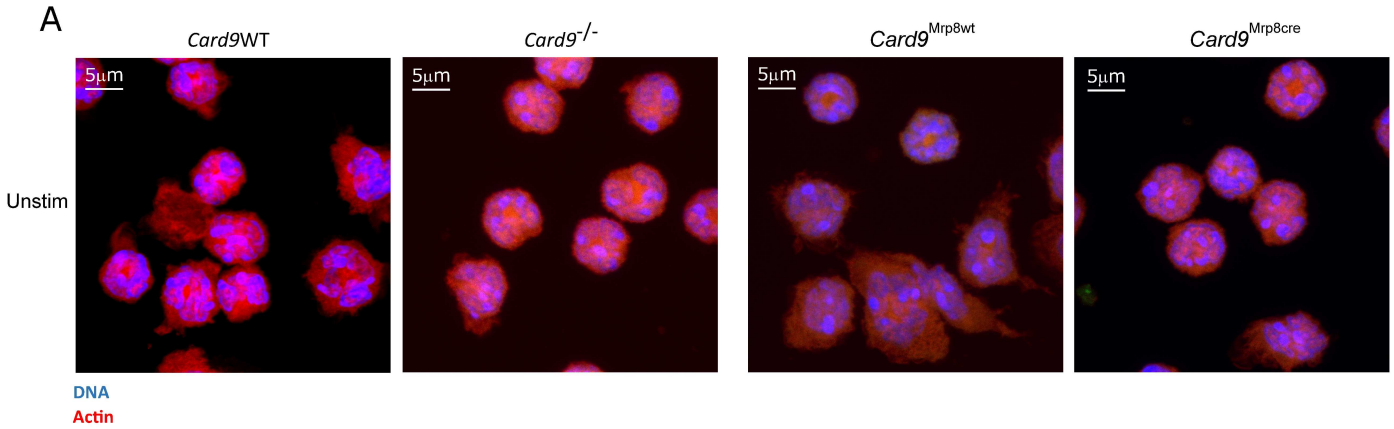
A
Card9WT
Card9-/-
Card9Mrp8wt
Card9Mrp8cre
5µm
Unstim
DNA
Actin

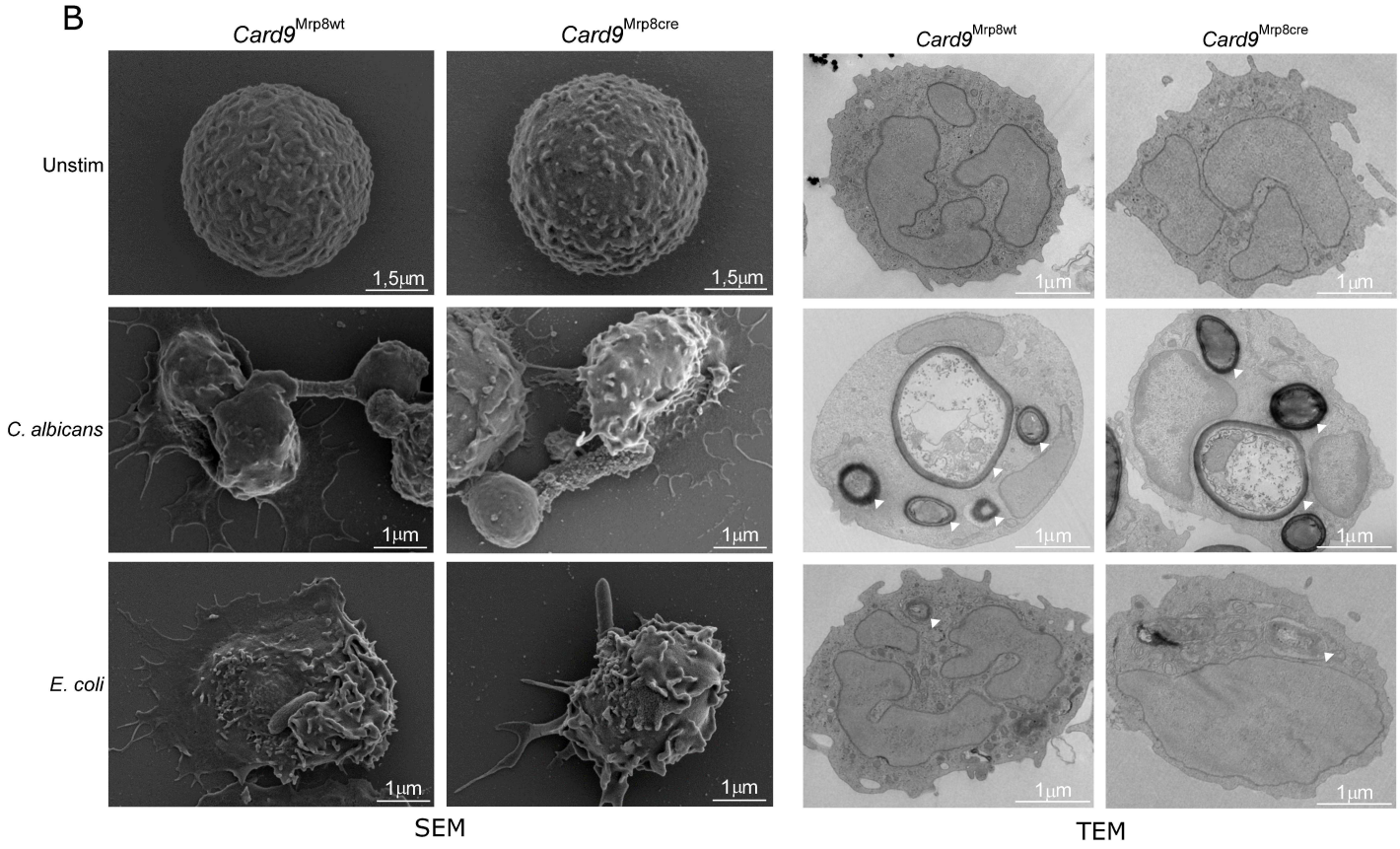
B
Card9Mrp8wt
Card9Mrp8cre
Card9Mrp8wt
Card9Mrp8cre
Unstim
C. albicans
E. coli
1,5µm
1µm
SEM
TEM

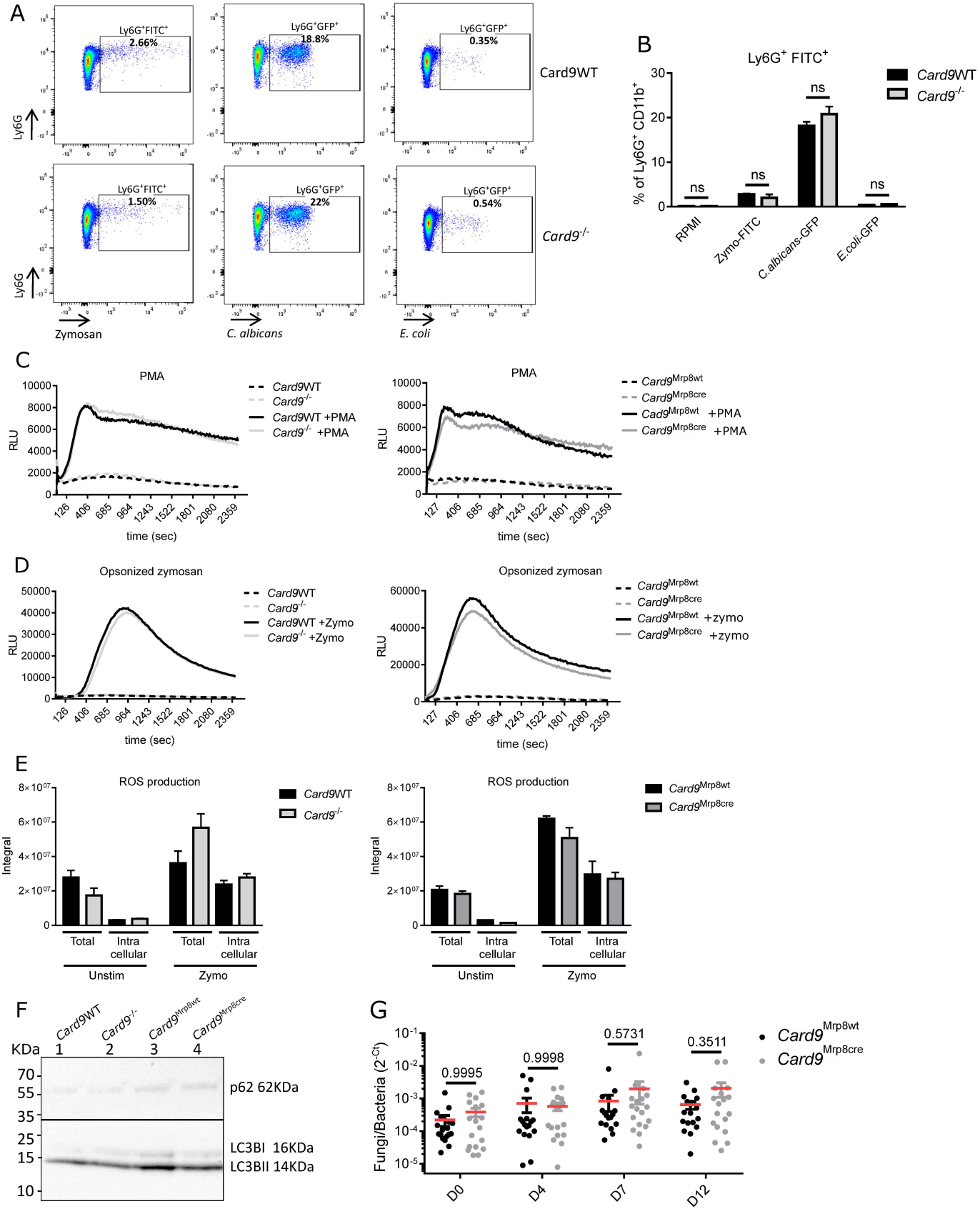
A
Ly6G+FITC+ 2.66%
Ly6G+GFP+ 18.8%
Ly6G+GFP+ 0.35%
Card9WT
Ly6G+FITC+ 1.50%
Ly6G+GFP+ 22%
Ly6G+GFP+ 0.54%
Card9-/-
Ly6G
Zymosan
C. albicans
E. coli
B
Ly6G+ FITC+
% of Ly6G+ CD11b+
Card9WT
Card9-/-
ns
RPMI
Zymo-FITC
C.albicans-GFP
E.coli-GFP
C
PMA
RLU
time (sec)
Card9WT
Card9-/-
Card9WT +PMA
Card9-/- +PMA
Card9Mrp8wt
Card9Mrp8cre
Cad9Mrp8wt +PMA
Card9Mrp8cre +PMA
D
Opsonized zymosan
Card9WT +Zymo
Card9-/- +Zymo
Card9Mrp8wt +zymo
Card9Mrp8cre +zymo
E
ROS production
Integral
Total
Intra cellular
Unstim
Zymo
F
KDa
p62 62KDa
LC3BI 16KDa
LC3BII 14KDa
G
Fungi/Bacteria (2-Ct)
0.9995
0.9998
0.5731
0.3511
D0
D4
D7
D12
H

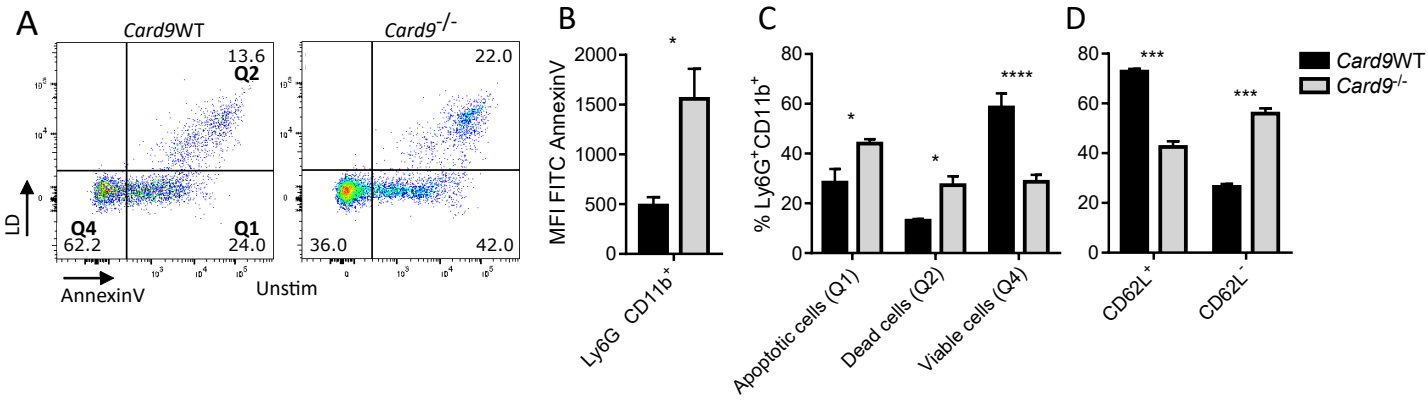
A
Card9WT
Card9-/-
13.6
Q2
22.0
Q4
62.2
Q1
24.0
36.0
42.0
LD
AnnexinV
Unstim
B
MFI FITC AnnexinV
2000
1500
1000
500
0
*
Ly6G+ CD11b+
C
% Ly6G+CD11b+
80
60
40
20
0
*
*
****
Apoptotic cells (Q1)
Dead cells (Q2)
Viable cells (Q4)
D
80
60
40
20
0
***
***
CD62L+
CD62L-
Card9WT
Card9-/-

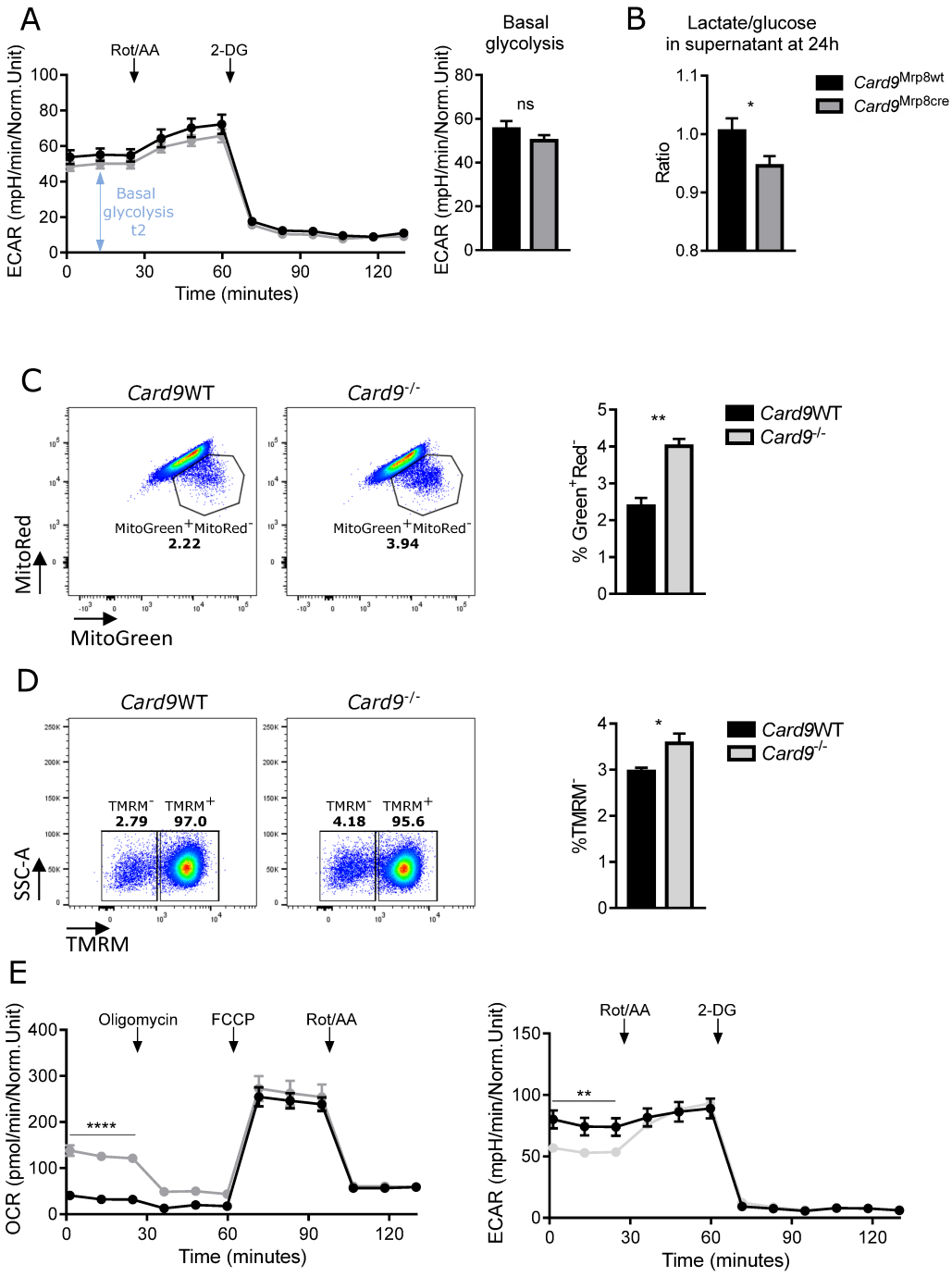
A
Rot/AA
2-DG
ECAR (mpH/min/Norm.Unit)
Basal glycolysis t2
Time (minutes)
Basal glycolysis
ns
B
Lactate/glucose in supernatant at 24h
Ratio
Card9Mrp8wt
Card9Mrp8cre
C
Card9WT
Card9-/-
MitoGreen+MitoRed-
2.22
3.94
MitoRed
MitoGreen
% Green+Red-
D
TMRM-
TMRM+
2.79
97.0
4.18
95.6
SSC-A
TMRM
%TMRM-
E
Oligomycin
FCCP
Rot/AA
OCR (pmol/min/Norm.Unit)
Time (minutes)
2-DG

Table S1. Histological grading of colitis

Feature graded	Grade	Description
Inflammation severity	0	None
	1	Slight
	2	Moderate
	3	Severe
Inflammation extent	0	None
	1	Mucosa
	2	Mucosa and submucosa
	3	Transmural
Crypt damage	0	None
	1	Basal 1/3 damaged
	2	Basal 2/3 damaged
	3	Only surface epithelium lost
	4	Entire crypt and epithelium lost
Percent involvement	1	1-25%
	2	26-50%
	3	51-75%
	4	76-100%

For each feature, the product of the grade and the percentage involvement was established. The histological score was obtained by adding the subscores of each feature.

Table S2 List of oligonucleotides and antibodies

Oligonucleotides	**SEQUENCE/SOURCE**	**IDENTIFIER**
Gapdh (sense)	AAC TTT GGC ATT GTG GAA GG	
Gapdh (antisense)	ACA CAT TGG GGG TAG GAA CA	
*Card9*exon1F (sense)	CAG TGA CCC CAA CCT GGT CAT	
*Card9*exon3R (antisense)	TCT GCA GCT TCA TGA CCT CTG TC	
All fungi (sense) (ITS1, ITS2)	CTT GGT CAT TTA GAG GAA GTA A	
All fungi (antisense) (ITS1, ITS2)	GCT GCG TTC TTC ATC GAT GC	
All bacteria (sense) (16s)	CGG TGA ATA CGT TCC CGG	
All bacteria (antisense) (16s)	TAC GGC TAC CTT GTT ACG ACT T	
All bacteria (Probe) (16s)	6FAM-CTT GTA CAC ACC GCC CGT C-MGB	
Il-23 mouse (sense)	AGC GGG ACA TAT GAA TCT ACT AAG AGA	
Il-23 mouse (antisense)	GTC CTA GTA GGG AGG TGT GAA GTT G	
Lcn2 mouse	Quantitect	Mn_Lcn2_1_SG QT00113407
Cxcr2 mouse (sense)	CTC ACA AAC AGC GTC GTA GAA C	
Cxcr2 mouse (antisense)	AGG GCA TGC CAG AGC TAT AAT	
S100a8 mouse (sense)	TCA AGA CAT CGT TTG AAA GGA AAT C	
S100a8 mouse (antisense)	GGT AGA CAT CAA TGA GGT TGC TC	
Antibodies		
CARD9 (A-8)	Santa Cruz Biotechnology	Cat# sc-374569
β-ACTIN (D6A8)	Cell Signaling Technology	Cat# 8457S
APC-labeled anti-mouse TCRγδ (GL3)	eBioscience	Cat# 17-5711-82
anti-CD16/32 (93)	eBioscience	Cat# 14-0161-85
PerCP5.5-labeled anti-mouse CD45 (30-F11)	eBioscience	Cat# 45-0451-82
FITC–labeled anti-mouse CD3ε (145-2C11)	eBioscience	Cat# 11-0031-85
BV605-labeled anti-mouse CD8α (53-6.7)	BioLegend	Cat# 100744
PE-labeled anti-mouse CD4 (RM4-5)	eBioscience	Cat# 12-0042-83
AF700-labelled CD19 (6D5)	BioLegend	Cat# 115528
PE-labelled CD11c (N418)	BioLegend	Cat# 117308
APC-labelled F4/80 (BM8)	BioLegend	Cat# 123116
AF700-labelled CD11b (M1/70)	BioLegend	Cat# 101222
APCFire750-labelled CD45 (30-F11)	BioLegend	Cat# 103154
PerCP5.5-labelled Ly6G (1A8)	BioLegend	Cat# 127616
PE-labelled CD11b (M1/70)	eBioscence	Cat# 12-0112-82
BV421-labelled CD62L (MEL-14)	BioLegend	Cat# 104424

Table S3. Characteristics of IBD patients

	Control IBD patients	CARD9 IBD patients	Healthy subjects
Number	11	8	6
Age (years)	40.5 ±8	48 ±7.6	33.7 ±5.9
% Male	5 (55.5%)	4 (50%)	2 (33.3%)
Treatment			
oral-5-ASA (%)	4 (36%)	2 (25%)	0
anti-TNF (%)	10 (90%)	7 (87.5%)	0
anti-integrin a4b7 (%)	1 (10%)	1 (12.5%)	0
methotrexate (%)	2 (18%)	1 (12.5%)	0

Cohort characteristics in terms of age, sex and treatment. Numeric data are summarized as mean ± s.d.

Sampling and analysis performed between 01/2022 and 04/2022.